1-31-1990

Investigation of the fluid dynamics of bioprosthetic heart valves

Carol A. Calta
New Jersey Institute of Technology

Copyright Warning & Restrictions

The copyright law of the United States (Title 17, United States Code) governs the making of photocopies or other reproductions of copyrighted material.

Under certain conditions specified in the law, libraries and archives are authorized to furnish a photocopy or other reproduction. One of these specified conditions is that the photocopy or reproduction is not to be "used for any purpose other than private study, scholarship, or research." If a, user makes a request for, or later uses, a photocopy or reproduction for purposes in excess of "fair use" that user may be liable for copyright infringement,

This institution reserves the right to refuse to accept a copying order if, in its judgment, fulfillment of the order would involve violation of copyright law.

Please Note: The author retains the copyright while the New Jersey Institute of Technology reserves the right to distribute this thesis or dissertation

Printing note: If you do not wish to print this page, then select "Pages from: first page # to: last page #" on the print dialog screen

ABSTRACT

Title of Thesis: Investigation of the Fluid Dynamics of Bioprosthetic Heart Valves

Carol A. Calta, Master of Science, 1989

Thesis directed by: Dr. Piero Armenante, Assistant Professor

There is a strong connection between altered arterial blood flow and vascular disease. The presence of disturbed flow and/or excessive turbulence is an indication of an abnormality within the cardiovascular system. The examination of cardiovascular fluid dynamics provides insights into the working of the cardiovascular system and ways to improve the design of implantable bioprosthetic valve designs. This investigation examines the fluid flow of arterial systems, and ways to apply this knowledge to the valves implanted into patients.

This thesis involves an investigation of the testing of bioprosthetic valves within simulated left heart flow loops. These systems include pulse duplicators and accelerated fatigue testers. Several variations of an arterial pulse pressure model are analyzed. These models numerically simulate arterial flow and pressure through electrical analog circuits, incorporating resistance, capacitance and inertia parameters. The governing fluid flow equations for an oscillating fluid are examined, for laminar and turbulent flow, and an exact solution to the Navier-Stokes equation is

calculated for an incompressible, laminar, Newtonian fluid with an imposed periodic pressure gradient. This solution can be used for comparison with experimental results. A program was created for data analysis to be used in conjunction with a Laser Doppler Velocimeter system that measures fluid velocity downstream of a bioprosthetic valve within a left heart simulator. The methods used to analyze the flow measurements are also discussed, with emphasis placed upon techniques applicable to pulsatile flow situations.

2) INVESTIGATION OF THE FLUID DYNAMICS

OF BIOPROSTHETIC HEART VALVES

1)

by Carol A. Calta

Thesis submitted to the Faculty of the Graduate School of the
New Jersey Institute of Technology in partial fulfillment of
the requirements for the degree of
Master of Science in Biomedical Engineering
1989 90

APPROVAL SHEET

Title of Thesis: Investigation of the Fluid Dynamics of Bioprosthetic Heart Valves

Name of Candidate: Carol A. Calta
Master of Science, 1990

Thesis and Abstract Approved: _____ Jan 10, 1990

Dr. Piero Armenante
Assistant Professor
Chemical Engineering
Date

_____ 1/10/1990

Dr. David Kristol
Professor
Chemical Engineering
Date

_____ 1/10/1990

Dr. Peter Engler
Associate Professor
Electrical Engineering
Date

VITA

Name: Carol A. Calta.

Permanent Address:

Degree and date to be conferred: Master of Science, 1989.90

Date of birth:

Place of birth:

Secondary education: Seton Catholic Central H.S., 1978.

Collegiate institutions attended:

New Jersey Institute of Technology	1988-1989	Master of Science

Major: Biomedical Engineering

von Kármán Institute for Fluid Dynamics	1985-1986	Diploma Course

Major: High Speed Fluid Dynamics

State University of New York at Buffalo	1978-1982	Bachelor of Science

Major: Aerospace Engineering

Publications: LDV Measurements in a High Speed Boundary Layer, VKI Project Report 1986-18.

Positions Held:

8/89 - present: Thermal Engineer
GE Astro Space
P.O. Box 800
Princeton, NJ.

12/84 - 1/88 : Flight Engineer
Singer Link Flight Simulation
Binghamton, NY.

2/83 - 12/84 : Engineer
McDonnell Douglas Aircraft Company,
St. Louis, MO.

TABLE OF CONTENTS

LIST OF TABLES

LIST OF FIGURES

INTRODUCTION

There is a strong connection between altered arterial blood flow and vascular disease. The presence of disturbed flow and/or excessive turbulence is an indication of an abnormality within the cardiovascular system. The examination of cardiovascular fluid dynamics provides insights into the working of the cardiovascular system and ways to improve the design of implantable bioprosthetic valve designs. This investigation examines the fluid flow of arterial systems, and ways to apply this knowledge to the valves implanted into patients.

Due to the unique characteristics of blood flow, numerical and computational representations are often unable to provide accurate information regarding the arterial flow system. Thus it is often necessary to perform experiments in order to fully comprehend the workings of this complex system. The fluid dynamics of aortic blood flow is very complicated. The flow is unsteady, viscous and often turbulent. The velocity profiles are a function of time, as are the shear rates, due to the pulsatile nature of the fluid flow. In the case of a non-Newtonian fluid, such as blood, the viscosity is a function of the rate of shear, which is constantly in a state of flux. The vessel walls containing the fluid are compliant, taper, and bifurcate. Due to the non-static nature of the bounding walls, it may be possible that the "no slip" condition does not exist within arterial vessels, thus

further complicating this already dynamic flow field. Also, there exists the intricate nature of entry flow, whereby the boundary layers are not fully developed. In addition, studies have shown that the amount of erythrocytes within the blood influences the intensity of turbulence (Ref. 47). These are just a few of the details that show the complexity of analyzing the fluid dynamics of blood flow.

Bioprosthetic valves were initially designed with the objective of simulating the natural blood flow of a healthy human valve. Comparatively, their predecessors, mechanical valves, do not exhibit realistic flow characteristics but do have the advantage of long term durability. To date, the bioprosthetic valves have been unable to improve greatly upon the durability aspect (Ref. 4, 42, 53 and 54). However, they do not promote thrombosis, and do not require long term anticoagulation therapy. Many different types of studies are being performed to elucidate the fatigue strength of bioprosthetic valves, as will be discussed within this essay.

Investigations can be performed either in vivo or in vitro. In vivo tests yield the most accurate results; however there could be risk to human life along with great expense and inconvenience. The use of mock circulatory systems enables researchers to investigate the fluid dynamics of the cardiovascular system without the disadvantage of human risk. These experimental systems, such as pulse duplicators, are used to test bioprosthetic heart valves in a environment that mimics the left heart. Pressure and flow measurements are

used to investigate the properties of valves for comparison and design improvement. More advanced techniques, such as Laser Doppler Velocimetry, Hot Film and Wire Anemometry, Doppler Ultrasound and Flow Visualization, provide more detailed information such as velocity profiles, shear stresses and turbulence intensities. Accelerated mock systems are used to test the long term durability of valves and can also utilize these advanced measurement techniques for flow field evaluation. However, the results from these tests are only as good as the system used. In order to fully understand the fluid dynamics of arterial blood flow it is necessary to incorporate several degrees of detail into an experimental model, such as distensible boundaries and vessel geometry. For the time being these factors are formidable.

This thesis involves an investigation of the testing of bioprosthetic valves within simulated left heart flow loops. These systems include pulse duplicators and accelerated fatigue testers. Several variations of an arterial pulse pressure model are analyzed. These models numerically simulate arterial flow and pressure through electrical analog circuits, incorporating resistance, capacitance and inertia parameters. The governing fluid flow equations for an oscillating fluid are examined, for laminar and turbulent flow, and an exact solution to the Navier-Stokes equation is calculated for an incompressible, laminar, Newtonian fluid with an imposed periodic pressure gradient. This solution can be used for comparison with experimental results. A

program was created for data analysis to be used in conjunction with a Laser Doppler Velocimeter system that measures fluid velocity downstream of a bioprosthetic valve within a left heart simulator. The methods used to analyze the flow measurements are also discussed, with emphasis placed upon techniques applicable to pulsatile flow situations.

TESTING OF BIOPROSTHETIC HEART VALVES

1. DISCUSSION OF VALVES

The evaluation of the long term durability of bioprosthetic heart valves is essential to optimizing the design and development of these devices. Since the introduction of prosthetic heart valves, studies have been performed in order to elucidate the factors that contribute to their failure. The initial valves used were mechanical valves. These devices are classified as the caged-ball, caged-disk and tilting-disk types. The mechanical valves are still in use today, exhibiting long term durability (Ref. 56). However, this advantage is overshadowed by poor hemodynamics, high rate of thromboembolism, occurrences of tissue overgrowth and the necessity of continuous anticoagulation therapy (Ref. 19). Within the past few years biological heart valves have been introduced, with the objective of overcoming the poor characteristics of the mechanical valves while still maintaining their durability traits. Biological heart valves exhibit more realistic flow characteristics as compared to the mechanical valves. Also, they do not promote acute thrombosis, nor is continual anticoagulation therapy necessary.

Bioprosthetic valves consist of either a porcine valve or bovine pericardium shaped into a valve, which is mounted onto flexible frame or stent. This stent reinforces the valve,

allowing it to maintain its shape and also facilitates its implantation into the patient. The frame is made of a corrosion resistant alloy and is covered by a porous, knitted fabric (usually Dacron or polytetrafluoroethylene) which theoretically will promote tissue ingrowth. Usually the valve consists of three cusps, although Meadox Medical (Ref. 23) has developed a unicusp valve. The proper functioning of these cusps is vital to the circulation of oxygenated blood to the body. The valves are stored in a solution of glutaraldehyde, which preserves and stabilizes the tissue (Ref. 2). There are numerous types and sizes of bioprosthetic valves produced by several companies.

Complications arise due to residual pressure gradients, thromboembolism formation, hemolysis, infection and problems associated with anticoagulation. A majority of clinical evaluations cite degeneration of bioprosthetic heart valves to be the main cause of failure. Degeneration, according to The Bantam Medical Dictionary (Ref. 3), is the "deterioration and loss of specialized function of cells of a tissue or organ. The changes may be caused by a defective blood supply or by disease." In essence, degeneration is a catch-all term used in respect to bioprosthetic heart valves to indicate failure due to immunological problems, foreign body reactions, blood-surface interactions, chemical factors and infection. Calcification of the valve is the most common form of degeneration and is most commonly cited in medical journals as the predominant cause of bioprosthetic heart

valve failure. Within the last decade, bioengineers and physicians have been focusing on the fluid dynamics of the valves, the role of mechanical factors and material fatigue as alternative sources of bioprosthetic heart valve failure. Studies have been performed in order to investigate the fluid stresses upon the valve, the flow profiles upstream and downstream of the valve, the stress factors of the bending areas of the cusps, the contact surfaces to which the cusps bend, the materials constituting the valves and other design factors.

2. PULSE DUPLICATORS

Researchers have developed fluid flow loops that simulate the flow of the left heart. These devices, known as pulse duplicators, contain chambers representing the left atrium and left ventricle, and a passage representing the aorta. Associated with the chambers are locations for mounting mitral and aortic valves. Pulse duplicators are used by physicians, bioengineers and manufacturers.

In the case of bioprosthetic valve fabrication, each valve is unique. The effective functioning of a valve must be accurately appraised before human implantation. Testing of each valve is performed by placing the valve into a pulse duplicator, using buffered glutaraldehyde as the working fluid. First, the valve is subjected to a physiological pressure gradient and observed for regurgitant flow. If the

valve does not have a considerable amount of back flow, the flow characteristics are then recorded within the pulse duplicator and the valve is prepared for human use.

Bioengineers and physicians utilize pulse duplicators to test new valve designs and modifications to existing valves. Normally, the flow simulator can operate under either steady or pulsed flow, where in the latter case the stroke volume and pulse rate can often be controlled. Tests yield valve characteristics such as effective orifice area, percent regurgitation, closing pressure and forward flow rate. With additional equipment it is possible to evaluate shear stresses, turbulence intensity, Reynold's stresses and much more valuable information, that can be used to assess the integrity of a valve design.

3. ACCELERATED TESTERS

For an average heart rate of 72 beats per minute, a natural heart valve cycles at approximately 38 million cycles per year. Consequently, the heart valve material is subject to repeated and fluctuating loads that lead to loss of strength, hardening and deterioration. Fatigue is "a general term used to describe the behavior of materials under repeated cycles of stress or strain which cause a deterioration of the material that results in a progressive fracture" (Ref. 40). It is clear that the heart valve is most certainly subject to fatigue and that fatigue testing is needed to assess the long

term behavior of implanted bioprosthetic heart valves. Fatigue failure is exaggerated in these valves because the tissue is nonliving and thus unable to rejuvenate itself as it is subjected to progressive deterioration.

Literature shows three types of tests used to analyze the durability of bioprosthetic heart valves. The first test consists of static tensile tests and accelerated fatigue tests used to examine the durability of the valve. In this type of experiment the material itself is tested, independent of the valve type, design, mounting and size (Refs. 7 & 8). The second type of experiment consists of clinical studies of valves implanted into laboratory animals. The subsequently explanted devices are then subjected to intense examination and compared to bioprosthetic valves explanted from humans (Refs. 4, 42, 53 & 54). The last type of fatigue analysis involves an accelerated fatigue tester which utilizes the entire valve. The experimental results are also compared with explanted human valves.

Several investigators have developed accelerated fatigue tester systems that involve the fatigue analysis of complete bioprosthetic heart valves, rather than solely the valve tissue (Refs. 19 & 44). The use of accelerated fatigue testing can yield useful information regarding the rate and mode of bioprosthetic failure in vivo. These systems, like the pulse duplicator, consist of an enclosed fluid that is propagated by a forward displacement pump. The chamber containing the test valve is often modeled to simulate the

geometry of the region containing the aortic valve. The tests are performed at rates of 1200 to 2100 cycles per minute, for up to 10^7 iterations or until the valve fails. The pressure gradient across the valve is measured with a sensitive pressure transducer and an electromagnetic flow meter is utilized to determine the simulated cardiac output. These measurements are done to insure that the systems pressure and volumetric flow rate are representative of the actual physiologic conditions. Although no direct stress or strain measurements are performed, these systems can be used in determining the length and mode of valve failure in an accelerated manner. Also, the stress factors of the cuspal bending areas, the contact surfaces to which the cusps bend, the durability of the valve frame and other design factors can be investigated. Valves that fail in fatigue testers can be utilized for in vitro analysis.

The fatigued valve can be placed within a pulse duplicator and with Laser Doppler Velocimetry (LDV) or Doppler Ultrasound techniques the flow characteristics of the fluid upstream, downstream and at the valvular cusps can be analyzed. From this type of experiment an analogy can be made with in vivo analyses (by comparing the flow data) to predict the state of a valve within the human body. Studies show (Ref. 20) that the bioprosthetic valves that fail in vitro also fail in vivo in the same fashion. Similarly, bioprosthetics that last longer in vitro also last longer in vivo. Researchers agree that the hemodynamics of biological

valves are superior to that of mechanical valves, and this is where the accordance ends. Accelerated fatigue testing systems have made it possible to produce in vitro cuspal tears and perforations similar to those occurring in vivo. But, since the testing occurs at high frequencies as compared to the actual heart rate, the movement of the valve may not correspond to the physiological motion. Considerations of fatigue testing system results must include frequency effects, temperature effects, the influence of the working fluid characteristics, and similarities of pressures and wave form shapes. Also, the absence of physiological tissue to fluid reactions must be incorporated into the interpretation of the results.

CARDIOVASCULAR FLUID DYNAMICS

1. BLOOD FLOW THROUGH LARGE ARTERIES

In order to properly investigate the fluid dynamics of bioprosthetic heart valves it is necessary to examine the properties of the working fluid - blood. Blood is a complex fluid that is composed of many specialized cells. It mainly consists of plasma (55% by volume) and formed elements (45% by volume) (Ref. 14). The formed elements are predominated by erythrocytes, also known as red blood cells, leukocytes and platelets. The density of the plasma is less than the density of the erythrocytes. Nevertheless, this proves to be insignificant when considering the working fluid within large arteries. Therefore, we can consider blood to be a homogeneous continuum with a specific gravity of 1.056. Even for turbulent flow the erythrocyte (diameter of approximately 8 μm) is much smaller than the smallest eddy size and thus the flow of blood in large arteries can be considered to be a continuum (Ref. 25). However, for decreasing vessel size, the prominence of the cell free layer of plasma near the vessel wall increases, disallowing the continuum approach. An important phenomenon that must be avoided is hemolysis, or rupture of blood cells. This occurs due to high shear stresses, turbulence, contact with rough surfaces and rapid pressure fluctuations. Great care must be taken when designing a prosthetic device to prevent such occurrences.

A Newtonian fluid is one that obeys the relationship :

$$\tau_{ij} = -\mu \left(\frac{du_i}{dx_j} \right) \qquad (1)$$

where, τ_{ij} : shear stress ($N\ m^{-2}$)

μ : viscosity ($kg\ m^{-1}\ s^{-1}$)

$\frac{du_i}{dx_j}$: fluid shear rate (s^{-1})

and viscosity is a physical property that characterizes the flow resistance of a fluid. Plasma is a Newtonian fluid, but whole blood is not. In the case of blood, the viscosity is not directly proportional to the ratio of shear stress to shear rate. Blood viscosity is a function of the shear rate, the amount of red blood cells within the blood and the flow conditions. A good representation of the stress-strain relationship of blood is rendered by Casson's equation (Ref. 16):

$$\tau_{ij}^{1/2} = \mu^{1/2} \left(\frac{du_i}{dx_j} \right)^{1/2} + Y_{ij}^{1/2} \qquad (2)$$

where, Y_{ij} is the yield stress, or the amount of shear stress that must be exceeded in order to have blood flow. The yield stress depends upon the amount of red blood cells present in the blood. For shear rates greater than 100 s^{-1}, as is the case in large arteries, blood viscosity is constant and can be considered to be Newtonian.

The characteristics of the vessel boundaries are also of concern. The vessel walls of the aorta are distensible. The arterial wall is an elastic body, whose motion is influenced by the constraints of the tissue in which it is embedded. This elasticity is important in maintaining forward fluid motion and also in attenuating pulse waves. Along with vessel distensibility, the vessel wall is tapered, contains curves, branches and irregularities.

Pulse duplicators and accelerated testers simulate the left heart using a working fluid that is analogous to blood (with respect to its density and viscosity). The tubes used to represent the left ventricle and the aorta are straight and rigid in most simulators. To compensate for their lack of compliance, distensible tubes are integrated into the system downstream of the aortic section. The design of these mock systems is initially modeled numerically with an arterial pulse pressure algorithm.

2. ARTERIAL PULSE PRESSURE MODEL

Left heart flow can be numerically simulated using arterial pulse pressure models. These models are essentially electrical analogs that use flow rate as the input and the arterial pressure wave as the output. They allow for arterial experimentation without the need for costly equipment and without risking human life. By simply altering certain parameters, tests can be performed to determine the

effects of changes from the norm, such as partial vessel occlusion to decreased blood flow rate. The important thing to keep in mind is the amount of complexity required in order to accurately represent the phenomena.

The earliest model of the arterial system was developed by Otto Frank in the late nineteenth century (Figure 1a). This model, known as the windkessel model, has been used to represent the aorta as an elastic air-chamber with an internal volume that is linearly proportional to the pressure. The remainder of the circulatory system is idealized by a linear resistor, representing the peripheral resistance of the arterial system. The compliance of the vessel is depicted by a capacitor, the pressure is analogous to the model's potential and the flow is represented by current. The windkessel model assumes that inertia is negligible and that the pressure wavelength is much larger than the characteristic length of the arterial system. It also assumes that the pressure on the venous side is equal to zero. Modifications of this model have been developed, incorporating inertia, vessel wall elasticity, and lumped models to represent the entire circulatory system (Refs. 9, 36, 49 & 50). Also models that incorporate the existence of pressure wave reflections have evolved, with in depth studies of their frequency range and input impedance.

3. ARTERIAL PULSE PRESSURE MODEL APPLICATIONS

This investigation examines the application of arterial pressure models, including the basic windkessel model (Model A), and modifications of this model, which shall be referred to as Models B, C, D and E (refer to Figure 1). All of the simulations are performed using DMSP (Discrete Model Simulation Program), which utilizes a fourth order Runge Kutta integration scheme (Ref. 39). The input used is the volumetric flow rate, which is proportional to the ratio of stroke volume and systolic interval. Referring to Figure 2, as the heart beats the ventricle contracts, ejecting a pulse of flow. The flow rate is harmonic, consisting of a pulse of flow, known as systole, and then a period of rest, known as diastole. During the simulation the stroke volume, systolic interval and heart rate can be modified to represent different conditions.

As was previously stated, the windkessel model makes several assumptions. In spite of these simplifications the model is quite reliable in yielding a realistic pressure wave (Figure 3), as produced from the DMSP program. This model can be used to simulate hypertension, altered peripheral resistance and alterations in vessel compliance, by properly modifying the appropriate parameters. Figure 3 shows the relationship between the volumetric flow rate (ml/s) and the pressure wave (mm Hg) with respect to the time evolved. The

pressure increase slightly lags behind the systolic flow input and is consistent with clinical measurements.

The major factor in properly simulating the arterial pulse pressure system is determining the parameters used to represent the system resistance, compliance and inertia. It is necessary to utilize physiological and anatomical properties in order to generate suitable initial values for these parameters. Resistance (R) can be determined by measuring the mean arterial pressure difference and cardiac output (volumetric flow rate). The ratio of these two quantities yields the peripheral resistance (Ref. 36). The compliance of a vessel wall (C) is determined by analyzing the change in volume with respect to the mean arterial pressure difference. Finally, the inertia term (L) can be determined by utilizing the ratio of the mean pressure difference with respect to the volumetric flow acceleration.

Several experimenters have performed clinical studies to ascertain these parameters using various techniques (Ref. 9, 36, 49 and 50). It is important to be aware of the fact that the experimentation techniques may alter the true value, for example by disturbing the flow. Also, one must rely on the accuracy and reproducibility of the equipment being used.

A mathematical approach can be utilized for parameter determination (for insertion into the DMSP module) which is based upon anatomical geometry, blood properties and vessel rheology. The parameters are related by:

$$R = \frac{8 \mu l}{\pi r^4} \qquad (3)$$

$$L = \frac{p l}{S} \qquad (4)$$

$$C = \frac{3 S (1+h)^2 l}{E (1+2h)} \qquad (5)$$

where, r = vessel outer radius (m)

p = blood density (kg m^{-3})

l = length of vessel segment (m)

S = vessel cross sectional area (m^2)

h = outer radius / wall thickness

E = Young's modulus of elasticity (kg m^{-2})

The value for resistance (Equation 3) is determined from the Hagen-Poiseuille law for steady flow through a circular tube (which will be described in detail later).

For the present simulations of the aforementioned models, initial values for the compliance and the main resistance were set equal to unity, utilizing the medically recognized units of mm Hg and ml. The inertia terms for Model D and Model E were comparably small (0.001 and 0.005 mm Hg s^2/ml, respectively). Initial tests were made, and the parameters were adjusted by trial and error to yield results that compared satisfactorily with in vivo data.

All of the simulations were evaluated using a time increment of 0.05 seconds, except for Model E, which required a much smaller time increment. Model B includes an additional resistor (R') to represent the characteristic

impedance of the aorta. This accounts for the higher frequency components of the pulse wave which are reflected and usually do not reach the major arteries due to these reflections. Figure 4 shows the results of Model B with C = 0.666 ml/mm Hg,
R = 1.25 mm Hg s/ml and R' = 0.075 mm Hg s/ml. The amplitude of the pressure wave is quite high, with a systolic pressure exceeding 160 mm Hg and a diastolic pressure of 80 mm Hg. By increasing the capacitance and slightly decreasing the main resistance, the systolic pressure is reduced considerably (Figure 5). Further increase in the capacitance (Figure 6) improves the pressure wave form and amplitudes. Figure 6 displays a normal pressure difference, although there is a lack of definition with respect to the pressure incisura. This simulation also provides a more realistic definition of the arterial pressure wave shape.

Model C is similar in content to Model B, differing only in structure. The resultant pressure waveform is similar, except that the peak systolic pressure is a higher, once the model has reached a steady state condition. It is interesting to note that a simple relocation of a parameter within a model can make an appreciable difference in the models output (Figure 7). Model D consists of the basic windkessel model with an added parameter to account for inertia. The inclusion of the acceleration term (inertia) yields a fuller waveform with a decreased difference between the diastolic and systolic pressures (Figure 8). The last

model tested, Model E, displayed a distinct dependence on the chosen time increment, and requires a more advanced integration technique to yield useful results. According to Toy, Melbin and Noordergraaf (Ref. 50), this model displays the most realistic behavior, without a gross increase in complexity.

These arterial pulse pressure models are essential in designing and properly utilizing pulse duplicators and accelerated testers. The desired resistance, compliance (or capacitance) and inertia can be calculated and mathematically modeled and then incorporated into these actual flow experiments. By fine tuning the values and locations of the parameters it is possible to create a reliable experimental device that can be used to investigate many aspects of arterial fluid flow.

4. DYNAMIC SIMILARITY

When modeling an actual fluid phenomenon for experimental purposes, it is necessary to ensure dynamic similarity. According to Schlichting (Ref. 43), two fluid motions are similar when at all geometrically mutual points the forces acting on a fluid particle have a fixed ratio at every instant of time. That is, the flows have geometrically similar streamlines. This is important in the field of arterial fluid dynamics, especially when using modified aortic geometries, fluids other than blood and increased

pulse frequencies as in the case of accelerated testing.

For pulsatile flows there are two nondimensional parameters that must be maintained in order to properly represent the fluid dynamics of the flow and to yield meaningful results. These parameters envelope the inertia forces, the friction forces and the frequency of oscillation.

The Reynold's number represents the ratio of the inertia force to the friction force and is always of significance for any fluid experiment. The Reynold's number based on vessel diameter is:

$$Re_d = \frac{\rho U d}{\mu} = \frac{U d}{\nu} \quad (6)$$

where, d = vessel diameter (m)

U = free stream velocity (m s^{-1})

ν = kinematic viscosity (m^2 s^{-1})

Similarly, the parameter characterizing a dimensionless frequency is known as the Strouhal number:

$$St = \frac{f d}{U} \quad (7)$$

where, f represents the frequency of the flow oscillation.

In reference to literature in the field of cardiovascular fluid dynamics, a nondimensional representation known as the Womersley parameter is utilized to indicate the frequency of

oscillation. The Womersley parameter is:

$$\alpha = R\ (f/\nu)^{1/2} \qquad (8)$$

where, R is the vessel radius. This parameter is actually a modified Reynold's number of a vessel with radius R, based on the flow frequency, as can be seen from the next equation.

$$\alpha^2 = Re_R\ St = \left(\frac{U\ R}{\nu}\right)\left(\frac{f\ R}{U}\right) \qquad (9)$$

The importance of this parameter will become evident later in this report when the investigation of oscillating pipe flow is taken into consideration.

5. GOVERNING EQUATIONS

It is necessary to examine the governing equations to obtain a good comprehension of the fluid dynamics of arterial blood flow. Assuming an incompressible, continuous fluid, the conservation of mass equation is:

$$\nabla \cdot \mathbf{u} = 0 \qquad (10)$$

and the conservation of momentum is:

$$\rho \frac{D\mathbf{u}}{Dt} = -\nabla P - (\nabla \cdot \tau) + \rho\ \mathbf{g} \qquad (11)$$

(a) (b) (c) (d)

where (a) is the mass per unit volume times the acceleration, (b) is the pressure force term, (c) is the viscous force term and (d) is the gravitational or body force term.

As previously stated, arterial fluid flow can be considered to be Newtonian and thus we can utilize the following expressions for the shear terms (τ).

$$\tau_{ii} = -2\,\mu\,\frac{\delta u_i}{\delta x_i} + \frac{2}{3}\,\mu\,(\nabla \cdot \mathbf{u}) \tag{12}$$

$$\tau_{ij} = -\mu\left(\frac{\delta u_i}{\delta x_j} + \frac{\delta u_j}{\delta x_i}\right) \tag{13}$$

Therefore the conservation of momentum equation becomes the Navier-Stokes equation for an incompressible fluid:

$$\rho\,\frac{D\mathbf{u}}{Dt} = -\nabla P - \mu\,\nabla^2\,\mathbf{u} + \rho\,\mathbf{g} \tag{14}$$

The Navier-Stokes equation along with the conservation of mass yields four equations with four unknowns : the velocity components u_i, u_j, u_k and the pressure P, assuming known body forces. The solution of these four equations can be physically determined with appropriately specified initial and boundary conditions. It should be noted here that only a handful of exact solutions to this set of equations exists. The remainder of problems need to be determined

experimentally or by rigorous numerical techniques.

In its simplest form, the aortic section can be considered as a pipe or tube with steady, laminar flow. One of the exact solutions of the Navier-Stokes equation is for steady, laminar, continuous flow of an incompressible, Newtonian fluid within a long pipe. This solution is known as the Hagen-Poiseuille law:

$$Q = \frac{\pi \, (P_{in} - P_{out}) \, R^4}{8 \, \mu \, L} \qquad (15)$$

where, Q = volume rate of flow ($m^3 \, s^{-1}$)

$P_{in} - P_{out}$ = pressure drop across the pipe ($N \, m^{-2}$)

L = pipe length (m)

This equation assumes that the flow is fully developed. The effects of inlet geometry and boundary layer growth are not considered.

6. EFFECTS OF ENTRANCE LENGTH

For a steady flow, the inlet geometry and the pipe Reynold's number (Re_d) are the important parameters affecting the entrance length (L_e), the length required for fully developed flow. Within the entrance region of a pipe, the boundary layer attached to the vessel wall has not yet converged and thus there is an inviscid core flow within the center of the vessel. The velocity profile appears flat near

the entrance and eventually develops as the distance from the entrance increases (see Figure 9). Since the boundary layer is thinner within the entry region, the wall shear stresses are larger due to increased velocity gradients. This increase in wall shear stress can lead to cell damage.

For a smooth inlet geometry, White (Ref. 55) has shown that for laminar pipe flow ($Re_d < 2300$):

$$\frac{L_e}{d} \approx 0.06\ Re_d \tag{16}$$

and for turbulent pipe flow ($Re_d > 2300$):

$$\frac{L_e}{d} \approx 4.4\ Re_d^{n} \tag{17}$$

where, d is the inner pipe diameter, and n is approximately 1/6.

Typically for blood in the aorta (Ref. 14):

$$\nu = \frac{\mu}{\rho} = 3.31\ 10^{-6}\ m^2\ s^{-1}$$

$$d \approx 0.026\ m$$

$$u_{peak} \approx 1.0\ m\ s^{-1}$$

$$Re_{d,peak} \approx 8000$$

and thus, $L_e/d \approx 20$. This estimate exceeds the value found from physiological geometries where the length from the

aortic valve to the lower thoraic artery divided by the average diameter is about ten to fifteen (Ref. 24), indicating that arterial flow is not fully developed. Thus we are unable to utilize the Hagen-Poiseuille law when modeling steady arterial flow, because the wall shear stresses will be much larger than those predicted by this law.

An additional degree of difficulty is added when considering oscillating flow. In this case the entrance length will fluctuate with time as a function of the pulsating flow. Due to the oscillations, flow as depicted by the Hagen-Poiseuille law will not occur unless the period of flow oscillation is much smaller than the development time of vorticity diffusion.

7. BOUNDARY LAYER EQUATIONS

Let us assume that the fluid is fully developed, for the sake of numerical analysis. This means that the Navier-Stokes equations can be simplified. Consider a two-dimensional flow, with only axial (z) and radial (r) velocity components. Fully developed pipe flow can be represented by the boundary layer equations, where it is assumed that the axial velocity is much greater than the radial velocity and that the gradients in the radial direction are much greater than those in the axial direction.

The flow can be laminar, transitional or turbulent.

Initially, a boundary layer will dèvelop in a laminar fashion, and then depending on the Reynold's number and the frequency of flow oscillation, become transitional and possibly turbulent. In the case of flow past a valve this phenomena becomes even more complicated by the jet-like effects upon the flow from the valve, the compliance of the vessel and regions of flow stagnation and recirculation. Within a laminar boundary layer the flow is smooth and the streamlines are parallel to the body surface. In turbulent boundary layer flow there occurs this general mean motion parallel to the body surfaces in addition to rapid and random velocity fluctuations. These fluctuations provide a mechanism for mixing within the turbulent boundary layer. Molecular movements within a laminar boundary layer yield viscous shear stresses. Within the turbulent boundary layer there are also turbulent, or Reynold's shear stresses.

Incorporating the properties of boundary layer flow within the Navier-Stokes equations yields the boundary layer equations for an unsteady flow in cylindrical coordinates.

$$z \text{ comp.} : \rho\left(\frac{\delta u_z}{\delta t} + u_r\frac{\delta u_z}{\delta r} + u_z\frac{\delta u_z}{\delta z}\right) = -\frac{\delta P}{\delta z} + \frac{\mu}{r}\left(\frac{\delta}{\delta r}\left(r\frac{\delta u_z}{\delta r}\right)\right) \qquad (18)$$

$$r \text{ comp.} : \frac{\delta P}{\delta r} = 0 \qquad (19)$$

For pipe flow this can be further reduced to:

$$\rho \frac{\delta u_z}{\delta t} = -\frac{\delta P}{\delta z} + \frac{\mu}{r}\left(\frac{\delta}{\delta r}\left(r\frac{\delta u_z}{\delta r}\right)\right) \qquad (20)$$

Although many of the previous assumptions still exist, these equations yield significant information about aortic flow.

8. OSCILLATING PIPE FLOW

By defining an oscillatory pressure gradient that induces pulsatile flow it is possible to determine the velocity profiles and shear stresses within a long cylindrical tube. An oscillating pressure gradient term can be defined as:

$$-\frac{1}{\rho}\frac{\delta P}{\delta z} = K \cos ft = \dot{K}\, e^{i f t} \qquad (21)$$

where, K is a constant. Examination of the continuity equation reveals that the axial velocity component is a function of the radial coordinate and time. Inserting the pressure gradient term into equation 20, and defining the boundary conditions such that there exists the no-slip condition at the wall, the solution for the axial velocity component can be found (see also Appendix A):

$$u_z = \text{Real}\left\{ \frac{-iK}{f} e^{i f t} \left(1 - \frac{J_0(\beta r)}{J_0(\beta R)} \right) \right\} \qquad (22)$$

where, J_0 is the Bessel function of the first kind and of zero order, and

$$\beta = (-i\ f/\nu)^{-1/2}$$

is comparable to the Womersley parameter divided by the radius. For low frequencies, the velocity profiles are parabolic and the flow oscillates in phase with the fluctuating pressure gradient. For higher frequencies, the fluid far from the wall moves as if it were frictionless and its phase is shifted with respect to the pressure gradient. The fluid elements near the wall undergo the greatest changes and the wall shear stress tends to lead the outer fluid. This results in a lagging of the core fluid behind the fluid near the walls. This phenomena can be explained by the fact that the fluid elements near the boundary have the lowest inertia, and are thus more susceptible to change, since they have less momentum (Ref. 24). The pressure gradient will have a more pronounced effect upon this slower moving fluid as compared to the core fluid, which has a greater momentum.

9. THE EFFECTS OF OSCILLATING FLOW ON TRANSITION

The main criterion used to numerically determine if a flow is laminar or turbulent is the Reynold's number. However, the Reynold's number itself is not a unique criterion. The level of incoming flow irregularity must be specified. For pipe flow, the critical Reynold's number (the value at which flow becomes transitional) is defined as 2300. In reality,

depending on the level of disturbance the critical Reynold's number can range anywhere between 2000 to 40,000 (Ref. 43). In turbulent flow there is a mixing process within the flow, and thus the velocity distribution becomes more distributed as compared to the parabolic laminar velocity profile. This distribution is due to the transfer of momentum, and there exists a random, three dimensional fluctuating field of vortices.

It is necessary to consider the effect of pulsatile flow on transition with respect to cardiovascular fluid dynamics, since the pressure gradient has an effect on the stability of the flow. Instead of specifying the Reynold's number as a function of the mean or free stream flow velocity as previously defined, a number of alternate determinations have been defined to incorporate the mean and fluctuating velocity components. For a fluctuating velocity distribution represented as:

$$u = U + u_f \cos ft \tag{23}$$

experiments have found that the critical Reynold's number depends only on the ratio of the fluctuating velocity (u_f) and the centerline velocity (U). Also, the length of transition (from onset of turbulence to fully turbulent) depends on the frequency of oscillation. An example for a non-steady Reynold's number (Re_{ns}) as proposed by Schlichting is:

$$Re_{rms} = \frac{u_* L}{\nu} \qquad (24)$$

where, L represents the characteristic length of the oscillating stream and is equivalent to the free stream velocity divided by the frequency of oscillation , so that,

$$Re_{rms} = \frac{U^2 \ (\ u_* \ / \ U \ )}{\nu \quad f} \qquad (25)$$

The ratio U/u_* represents the dimensionless amplitude of oscillation, and $f \nu / U^2$ represents the dimensionless frequency. These parameters are useful in indicating the onset of turbulence during experimentation since they incorporate not only the mean flow characteristics, but also the fluctuating ones.

10. TURBULENCE

Turbulence is an important phenomena in the field of cardiovascular fluid dynamics. In the human arterial system turbulence, as indicated by cardiac murmurs, or measured qualitatively by Doppler Ultrasound techniques, is significant with respect to aortic valvular disease. Subjects with an increase of flow disturbances in vivo, such as that due to stenoses, show a marked increase in turbulence intensity. Also, turbulent flow in the region of prosthetic heart valves has been shown to contribute to thrombus

formation, red cell destruction and valve deterioration.

The true nature of turbulence consists of a random fluctuation of pressure, velocity, vorticity that encompass a continuous spectrum of frequencies, such as white noise (Ref. 55). In the case of steady, turbulent flow the velocity consists of a steady, time independent term ($\bar{u}$) and a fluctuating component (u'), as is the case for the pressure term also.

$$u = \bar{u} + u' \tag{26a}$$

$$P = \bar{P} + P' \tag{26b}$$

The time independent term is defined by a time average:

$$\bar{u}_i = \frac{1}{T} \int_t^{t+T} u_i \, dt \tag{27}$$

where, T is the averaging time and should be sufficiently large to provide a realistic sample. Inserting these new terms for pressure and velocity into the Navier-Stokes equations (neglecting body forces) and utilizing the concept of Reynold's time averaging (Ref. 10) yields:

$$\rho \frac{Du}{Dt} = - \nabla P + \nabla \cdot \tau \tag{28}$$

where, $$\tau = \mu \left(\frac{\delta u_i}{\delta x_j} + \frac{\delta u_j}{\delta x_i} \right) - \rho \, u_i' u_j'$$

The first term of the stress matrix is the laminar viscous stress. The second term is the additional stress due to the fact that the flow is turbulent, and is known as the Reynold's stress. This second term is a nonlinear term representing the average transport of momentum per unit mass. The intensity of turbulence is a parameter used to indicate the extent of turbulence in a flow and is defined as:

$$I = \frac{(1/3 (\Sigma u_i'^2))^{1/2}}{U} \tag{29}$$

A problem arises when utilizing a time average scheme for unsteady flows. Ideally, the averaging time, T, should be large with respect to turbulent fluctuations and at the same time small with respect to the fluid mean motion variation. An alternate method, used for pulsatile flows, is the phase average. The components are defined as:

$$u = \bar{u} + \hat{u} + u' \tag{30}$$

with, $\langle u \rangle = \bar{u} + \hat{u}$

so that, $u = \langle u \rangle + u'$ (31)

The term $\bar{u}$ is once again the time mean, $\hat{u}$ is the statistical contribution of the periodic disturbance and u' is the turbulent component. The phase average $\langle u \rangle$ is defined as:

$$\langle u \rangle = \lim_{N \to \infty} \left(\frac{1}{N} \sum u(z, t+nT) \right) \tag{32}$$

where N is the number of cycles tested and T is the period of one cycle. This is analogous to an ensemble average where an average of values taken at the same time in different, repeated and uncorrelated experiments are used. The only difference being that for the phase average each cycle of period T is viewed as a separate experiment. This technique is only valid when there is extreme confidence that the period of each cycle is exactly the same as the previous cycle. This method can be used for periodically reliable pulse duplicators and accelerated testers, but is not valid in vivo, where the period from heart beat to heart beat is not identical. To determine the number of cycles to test experimentally, it is necessary to compute the phase average for a predetermined N, then repeat the test with a larger N. If the phase average does not change, then one is assured that the number of cycles being used is sufficient.

Incorporating the phase average technique into the Navier-Stokes equations yields a new definition, the phase averaged Reynold's stress term $-p\langle u_i' u_j' \rangle$, which represents the contribution of the turbulent field to the organized field. For all flow experiments measuring Reynold's stresses in

pulsatile simulations of arterial flow it is necessary to utilize a technique that does not combine the turbulent fluctuations with the periodic flow modulations, when determining the velocity components.

In many cases, it is not possible to create a perfectly repeatable flow due to phase irregularities. Within the arterial system, disturbed flow patterns grow and regress during a cycle and may contain coherent structures and oscillations in addition to the fluctuating turbulent components. Experiments investigating the spectral properties of turbulence (Ref. 28) have shown that the ensemble average technique may not properly eliminate the ensemble average waveform from the fluctuating component. This results in a underestimate of the Reynold's shear stresses (by approximately 25%) and thus a misjudgment of the actual effects of turbulence. This phenomena is most important early in the transition, to transitional-turbulent phases of flow development.

EXPERIMENTAL TECHNIQUES

Due to the complex nature of cardiovascular fluid dynamics, the primary emphasis of determining the flow characteristics through bioprosthetic heart valves is placed upon experimental techniques. Studies utilizing Laser Doppler Velocimetry (LDV) yield quantitative information without intruding upon the flow patterns. With this apparatus one can measure the velocity components, shear stresses, and turbulence intensity. The LDV system at NJIT consists of a Lexel 2 Watt argon ion laser and a TSI series 9100-7 LDV system (Figure 10). This system measures two velocity components (radial and axial) employing the dual beam fringe mode system with back scatter light collection. In Table 1 a complete list of laser and optical specifications can be found.

The experimental working fluid is seeded with small particles (that are compatible with the fluid) having a diameter of the order of 1 μ. These particles scatter light within the fringe pattern, which is created by the crossing of the laser beams at the point of measurement. This fringe pattern is located at the very center of the beam crossing, which is known as the probe volume. The scattered light is detected by the photomultipliers contained within the optical system (Figure 10). The output signals from the photomultipliers are sent to two TSI model 1990 signal processors (also referred to as counters). These processors

accept signals between 10mV to 2V peak to peak. Also, two Bragg cell frequency shifters are utilized for low or reversed velocity components. The information from the processors is passed to a NJIT personal computer via the TSI 1998K data converter. The 1998K data converter sends two 16 bit words per data point to the computer and the data is analyzed by a TSI software package (model 6235). The data can then be either stored, or used in a real time sampling display.

The real time option is used to optimize the optical system alignment and fine tune the position of the photomultiplier aperture with respect to the scattered light that contains the Doppler frequency (and thus velocity) information. However, this can only be done to one channel, and therefore one velocity component, at a time. The software displays a probability distribution function of the real time sample, indicating Doppler frequency with respect to number of data. Importance is placed upon maximizing the sampling rate in order to avoid false or biased measurements. Real time sampling enables the user to refine the laser system set-up, and is used as an aide in yielding reliable data results.

The 1998K data converter has several operating options that enable the user to control the amount, and type of data being sent to the computer for analysis. The signal processors are responsible for confirming the data points sent to the hardware from the photomultipliers. This is indicated by a data ready signal which is passed from the signal processors

to the data converter. The 1998K can either transfer data from the first counter that provides a valid data point, or transfer data only when a data ready signal is received from both processors within a user defined coincidence window. The first mode is known as the random mode, since data is sent to the computer whenever a data ready signal is detected. This mode does not allow for cross correlation between the two velocity components, disallowing the determination of Reynold's shear stresses since there is no connection between the axial and radial velocity components. The second mode, the coincidence mode, enables the defining of the turbulence parameters since data is sent from both signal processors within a predetermined coincident time. The validity of this information is a function of the width of the coincident window, which must be smaller than the smallest flow disturbance. The rate of desired data transfer is also controlled by the user, in increments of $2^n * 100\ \mu$ seconds. However, it is necessary to first have a data ready signal from the one or both of the counters in order to have a valid measurement.

The TSI software computes the mean velocity components, standard deviations, turbulence intensities, Reynold's shear stresses and a cross correlation coefficient, for a predefined number of data points. These computations are based on the Reynold's time averaging concept and thus are not applicable to pulsatile flow.

An interactive program has been written in FORTRAN, to

analyze the velocimeter information using the phase average technique (see Appendix B). This program consists of two sections, program DACQ and subroutine DEC2BIN. The internal subroutine DEC2BIN requests the name of the LDV data file and converts this data from a decimal format, as stored by the TSI software, back into binary format. Once this process is completed the binary information is written to another file, in the form of two 16 bit words per data point. The program DACQ then converts this data into logical information indicating the mode of operation of the 1998K data converter, and the Doppler frequency information.

The first word consists of bits indicating the mode of data acquisition, i.e. random mode or coincidence mode. This first word also contains a flag indicating the velocity component and the number of cycles (N) timed. The number of cycles indicates the number of fringes within the probe volume that a particle has passed through for the measurement, and is defined by the user as part of the signal processer set-up. The second word contains the time mantissa (t_m) and the exponent (exp). These parameters relate to the method that the counter times the passage of a particle through the fringe pattern, resulting in a Doppler frequency measurement and a data ready signal.

The final velocity measurement is then computed within program DACQ utilizing the following equation:

$$u_i = d_f * [(N * 10^9 / t_m * 2^{(exp-8)}) - f_m] \qquad (33)$$

where, d_f = fringe spacing (m)

f_m = frequency shift of the Bragg cell

The phase averaged velocity can be computed using equation 32. Since the background turbulence is random (by definition of turbulence), the fluctuating turbulent velocity components can be determined by:

$$u_i' = u_i - \langle u_i \rangle \tag{34}$$

therefore, it is possible to calculate phase average root mean square turbulence intensities:

$$(\langle u_i'^2 \rangle)^{1/2} = \left(\frac{1}{N} \Sigma \left(u_i'(t+nT)^2 \right) \right)^{1/2} \tag{35}$$

and the phase average Reynold's stresses:

$$\langle u_i' u_j' \rangle = \frac{1}{N} \left(\Sigma\, u_i'(t+nT)\, u_j'(t+nT) \right) \tag{36}$$

An attempt was made to perform an experiment upon a bioprosthetic valve within an accelerated fatigue testing system using the LDV system and software. The LDV system was assembled and tested, however, due to several difficulties, the experiment was not successfully completed.

DISCUSSION

Many LDV studies have been performed with pulse duplicators, investigating the flow through different types of valves. One such study (Ref. 17), investigating the wall shear stress distribution along the cusp of a tri-leaflet prosthetic heart valve, indicated that areas of increased surface shear stress enhanced the mechanical damage to the surface of the cusp. This study involved a two-dimensional LDV analysis of the flow along the moving boundary of the valve cusp. The results from this study, along with many others, show a direct relationship between wall shear stress and valve survivability. For high wall shear stresses, there is mechanical damage to the blood elements and mechanical failure of the valve due to cuspal surface damage. Low wall shear stresses indicate regions of flow stagnation or separation which is clinically linked to thromboembolism and tissue overgrowth.

When the valve cusps open unequally, the flow resembles asymmetric plug flow. The shear stresses differ along the cusps and the velocity profile downstream of the valve is non-uniform. Peak shear stresses correspond to the flexing of the cusps, since the rate of shear increases due to sudden changes in cuspal curvature. Einav (Ref. 17) found in his studies that peak wall shear stresses correspond to in vivo locations of calcific deposits, and to in vitro locations of extremely small decreases in bioprosthetic cuspal thickness.

LDV studies have also shown a decrease in wall shear stresses at the tips of the cusps, indicating boundary layer separation. The combination of increased shear stress at flexure points and decreased shear stress at separation points could accelerate deposition of platelets, calcium and other particles, and trigger thromboembolitic processes and calcification (Ref. 58). This theory is supported by clinical studies that correlate regions of high shear stresses to thrombus formations upon the cuspal surfaces (Ref. 42).

In vivo measurements of turbulence parameters have been made using Hot Film Anemometry (Ref. 47). This type of investigation analyzes the onset and duration of turbulence within human subjects. Patients with increased heart rate and stroke volume are found to have disturbances that commence earlier and last longer as compared to their healthy counterparts. In vitro investigations by these same researchers, show that maximum turbulence occurs at the tips of the valve cusps during flow ejection. The cusps trip the flow, causing it to become turbulent due to the fluttering of the leaflets of the valve. This is believed to also occur in vivo, due to weakening of the valve tissue.

Fluid dynamic studies have also been performed within accelerated testers. A highly sensitive pressure transducer is used upstream and downstream of the valve to determine the pressure gradient, and valve closing pressure. Figure 11 shows the results of such a measurement performed for this

thesis. The upstream pressure, downstream pressure and pressure gradient were measured within an accelerated fatigue test system containing a bovine pericardium bioprosthetic valve. During the period of forward flow, the upstream pressure is greater than the downstream pressure, as indicated by a positive pressure gradient. When the valve closes, there exists a phase where the flow is reversed. One of the measures of valve integrity is based upon the overall percentage of this regurgitant flow.

Recently, the technique of LDV has also been applied to determine the flow characteristics within accelerated testers (Ref. 44). It has been shown that the peak velocity through a bioprosthetic valve decreases early in the phase of the fatigue test due to the cyclic loading of the cuspal tissue. This supports the results ascertained from fatigue test experiments of the tissue alone, where the compliance of the tissue was found to slightly decrease in the early stage of the test and then remain constant. The flow information reaped from accelerated testers is questionable, since some failure modes obtained in vitro have no clinical correlation. Also, no effort has been made to maintain dynamic similarity within these testing devices. The working fluid usually has density and viscosity characteristics similar to water, and the Strouhal number is not preserved.

CONCLUSION

This thesis has shown the various methods used to examine the fluid flow through bioprosthetic heart valves. Analyzing arterial pulse pressure models provides insight into the parameters necessary to create a left heart flow simulator. Investigations of bioprosthetic valves within these mock circulatory loops provides vital information pertaining to the fluid flow through these valves. Proper analysis of the experimental results is necessary before the data can be interpreted and correlated with in vivo data and numerical computations. This analysis involves the use of a technique, such as the phase average ensemble in conjunction with the data processing program DACQ, to determine the various velocity components and the corresponding turbulence and shear stress parameters. With this information one can examine the shear stresses and flow characteristics that provide direct indications regarding valve competency.

It has been shown that high shear stresses, flow separation and turbulence decrease the overall durability of a bioprosthetic valve. High wall shear stresses yield mechanical damage to the blood elements. Regions of flow stagnation are indicated by low wall shear stresses, which are clinically linked to thromboembolism and tissue overgrowth.

Tests performed in vivo have shown that the onset and duration of turbulence coincides with valvular abnormalities,

such as weakened tissue, and calcium formation upon the valvular surfaces. Still, there is much work that needs to be done to increase the field of knowledge with respect to cardiovascular fluid dynamics and the effects of certain phenomena upon bioprosthetic valves. Experimentation within accelerated fatigue testers has the possibility of yielding such information, providing that the laws of dynamic similarity are maintained.

As for the causes that produce bioprosthetic valve failure, two theories have been proposed. According to Schoen and Hobson (Ref. 42), metabolic degeneration, primarily due to calcification, is the main cause of bioprosthetic heart valve failure. Walley et al (Ref.'s 53 and 54) and Einav (Ref. 17) instead proposed that mechanical and design factors are mainly responsible for these failures. It is possible that mechanical stress with consequent material breakdown and cuspal perforation may promote calcification. Also, intrinsic and extrinsic calcium deposits may weaken the cuspal architecture, leading to an eventual cusp rupture. It is the authors opinion that a combination of these factors leads to the ultimate failure of a bioprosthetic heart valve.

Regardless of these theories, the evidence that turbulent flow and high shear stresses are responsible for the degeneration and final failure of bioprosthetic heart valves has been proved by many experiments. It is now time to utilize this information in the modification and creation of new and more efficient bioprosthetic heart valves that can

endure many years of operational use while still maintaining a nondisturbed flow field.

There is a need for test standardization so that experiments can be compared. Cyclic rates, pressure differentials, flow rates, temperature, test section dimensions and test fluids need to be defined so that more information can be reaped from the tests being performed. Clinicians, numerical researchers, fluid dynamicists and accelerated fatigue test researchers need to combine their findings to produce coherent and well defined conclusions that will aid in an era of new and improved bioprosthetic heart valves.

APPENDIX A

OSCILLATING PIPE FLOW

For fully developed, laminar pipe flow of a Newtonian fluid...

Continuity equation :

$$\frac{1}{r}\frac{\delta}{\delta r}(r u_z) + \frac{\delta u_z}{\delta z} = 0$$

thus, u_z = function(r,t)

z - Momentum equation :

$$\frac{\delta u_z}{\delta t} = \frac{-1}{\rho}\frac{\delta P}{\delta z} + \nu \left[\frac{\delta^2 u_z}{\delta r^2} + \frac{1}{r}\frac{\delta u_z}{\delta r}\right]$$

Pressure Gradient term :

$$\frac{-1}{\rho}\frac{\delta P}{\delta z} = K \cos ft = K e^{ift}$$

recall that $e^{ift} = \cos ft + i \sin ft$

where, f = frequency
K = a constant

Boundary Conditions :

at r = 0.0 u_z is finite
at r = R $u_z = 0.0$

let, $u_z = g\, e^{ift}$ where g is a function of r only.

thus, $\frac{\delta u_z}{\delta t} = i f g e^{int}$

$\frac{\delta u_z}{\delta r} = g' e^{int}$ where ' denotes $\frac{\delta}{\delta r}$

$\frac{\delta^2 u_z}{\delta t^2} = g'' e^{int}$

z - momentum becomes :

$$g'' r^2 + g' r - \sigma g r^2 = -K r^2/v$$

where, $\sigma = i f/v$. This equation is similar to the Bessel Equation. By substituting :

$$s = r (-i f/v)^{-1/2} = r \beta \qquad \text{and,}$$

$$h(s) = h = g + iK/f$$

yields an exact form of the Bessel equation which can be solved for h :

$$h(s) = c_1 J_0(s) + c_2 Y_0(s)$$

applying the boundary conditions,

for $r = s = 0$ Y_0 is unbounded and thus $c_2 = 0$

for $r = R$, or $s = R \beta$ we find that

$$u_z = \text{Real} \left\{ \frac{-iK}{f} e^{i\omega t} \left(1 - \frac{J_0(r\beta)}{J_0(R\beta)} \right) \right\}$$

For small $R\beta$, such as is the case for slow oscillations :

$$u_z = \frac{K}{4v} (R^2 - r^2) \cos ft$$

the velocity distribution is in phase with the pressure gradient.

For large $R\beta$, such as is the case for fast oscillations :

$$u_z = \frac{K}{f} \left(\sin ft - (R/r)^{-1/2} e^{-\sqrt{(f/2v)}(R-r)} \sin(ft - \sqrt{(f/2v)}(R-r)) \right)$$

the fluid far from the wall moves in an inviscid manner and its phase is shifted with respect to the pressure gradient term.

APPENDIX B

```
      program dacq
cccc
cccc ccccccccccccccccccccccccccccccccccccccccccccccccccccccccccccccc
ccccccccccc
c
c       data conversion program
c
c       data consists of 2 words - read bits left to right
c
c       word 1 :  bit 1 - 1=more data            0=end of data
c                 bit 2 - 1=random mode          0=coincident mode
c                 bit 3 - time between samples   t=1 thru 14
c                 bit 4 -       "                t=15=handshake mode
c                 bit 5 -       "                del t = (2.**t)*100 micro sec
c                 bit 6 -       "
c                 bit 7 - not used
c                 bit 8 - 1=channel 1 (z)        0=channel 2 (r)
c                 bit 9 - N cycles
c                 bit 10-       "
c                 bit 11-       "
c                 bit 12-       "
c                 bit 13-       "
c                 bit 14-       "
c                 bit 15-       "
c                 bit 16-       "
c
c       word 2 :  bit 1 through 12 - time mantissa (timem)
c                 bit 13 through 16- exponent      (exp)
c
c       velocity = fringe space*[(N*1e09/(timem*2**(exp-3.)))-freq shift]
c
c
c
ccccccccccccccccccccccccccccccccccccccccccccccccccccccccccccccccccccc
      character*16 cbit1,cbit2,word(1024),fileo,cmode,fun,ctt
      real*8 delt(1024),fn(1024),timem(1024),exp(1024),
     .       fuc(1024),temp(1024)
      real*8 f211,f210,f29,f28,f27,f26,f25,f24,f23,f22,f21,f20
      real*8 fshftz,fshftr
      real*8 fringz,fringr,temuz,temuz2,temur,temur2
      real*8 meanuz,meanur,devuz,devur,turbiz,turbir,reystr,
     .       cxcor,tn,tt
      real*4 xloc,yloc,zloc
      integer*4 i,j,k,nsamp,nz,nr,ksamp
      common /ldvstuf/ fileo,nsamp,word,xloc,yloc,zloc,ksamp,
     .                 fshftz,fshftr
c
      data fringz/5.070e-06/
      data fringr/4.810e-06/
c
      data f211/2048./
      data f210/1024./
      data f29 /512./
      data f28 /256./
```

```
        data f27 /128./
        data f26 /64./
        data f25 /32./
        data f24 /16./
        data f23 /8./
        data f22 /4./
        data f21 /2./
        data f20 /1./

c
ccccccccccccccccccccccccccccccccccccccccccccccccccccccccccccccccccccccccc
c
        call dec2bin
c
c
c       open(12,file=fileo,status='old')
        write(*,'(a)')' new data file name - for velocities :'
        read(*,'(a)') fun
        open(13,file=fun,status='new')
        write(13,500)
c
c
        k =1
        nz=0
        nr=0
        temuz      = 0.0
        temuz2     = 0.0
        temur      = 0.0
        temur2     = 0.0
c
        do 100 i=1,ksamp,2
c
        delt(k)    = 0.0
        fn(k)      = 0.0
        timem(k)   = 0.0
        exp(k)     = 0.0
        fuc(k)     = 0.0
        temp(k)    = 0.0
c
        cbit1=word(i)
        cbit2=word(i+1)
c
        if(cbit1(2:2).eq.'0')then
          cmode='coincident'
        else
          cmode='random     '
        endif
c DELTA TIME BETWEEN MEASUREMENTS
        if(cbit1(3:3).eq.'1') temp(k) = temp(k) + f23
        if(cbit1(4:4).eq.'1') temp(k) = temp(k) + f22
        if(cbit1(5:5).eq.'1') temp(k) = temp(k) + f21
        if(cbit1(6:6).eq.'1') temp(k) = temp(k) + f20
        delt(k) = (2.0**temp(k))*100.e-06
c N CYCLE
        if(cbit1(9:9).eq.'1') fn(k) = fn(k) + f27
        if(cbit1(10:10).eq.'1') fn(k) = fn(k) + f26
```

```
         if(cbit1(11:11).eq.'1') fn(k) = fn(k) + f25
         if(cbit1(12:12).eq.'1') fn(k) = fn(k) + f24
         if(cbit1(13:13).eq.'1') fn(k) = fn(k) + f23
         if(cbit1(14:14).eq.'1') fn(k) = fn(k) + f22
         if(cbit1(15:15).eq.'1') fn(k) = fn(k) + f21
         if(cbit1(16:16).eq.'1') fn(k) = fn(k) + f20
c TIME MANTISSA
         if(cbit2(1:1).eq.'1') timem(k) = timem(k) + f211
         if(cbit2(2:2).eq.'1') timem(k) = timem(k) + f210
         if(cbit2(3:3).eq.'1') timem(k) = timem(k) + f29
         if(cbit2(4:4).eq.'1') timem(k) = timem(k) + f28
         if(cbit2(5:5).eq.'1') timem(k) = timem(k) + f27
         if(cbit2(6:6).eq.'1') timem(k) = timem(k) + f26
         if(cbit2(7:7).eq.'1') timem(k) = timem(k) + f25
         if(cbit2(8:8).eq.'1') timem(k) = timem(k) + f24
         if(cbit2(9:9).eq.'1') timem(k) = timem(k) + f23
         if(cbit2(10:10).eq.'1') timem(k) = timem(k) + f22
         if(cbit2(11:11).eq.'1') timem(k) = timem(k) + f21
         if(cbit2(12:12).eq.'1') timem(k) = timem(k) + f20
c EXPONENT
         if(cbit2(13:13).eq.'1') exp(k) = exp(k) + f23
         if(cbit2(14:14).eq.'1') exp(k) = exp(k) + f22
         if(cbit2(15:15).eq.'1') exp(k) = exp(k) + f21
         if(cbit2(16:16).eq.'1') exp(k) = exp(k) + f20
c CHANNEL 1(z) OR 2(r)
         if(cbit1(8:8).eq.'0')then
            nz=nz+1
            ctt=' z '
            fuc(k)=(fn(k)*1.e09/(timem(k)*(2.**(exp(k)-3.))))-fshftz
            fuc(k)=fringz*fuc(k)
            temuz=temuz+fuc(k)
            temuz2=temuz2+fuc(k)**2.
         elseif(cbit1(8:8).eq.'1')then
            nr=nr+1
            ctt=' r '
            fuc(k)=(fn(k)*1.e09/(timem(k)*(2.**(exp(k)-3.))))-fshftr
            fuc(k)=fringr*fuc(k)
            temur=temur+fuc(k)
            temur2=temur2+fuc(k)**2.
         endif
c
cccc     write(13,*)ctt,k,fuc(k),delt(k),fn(k),timem(k),exp(k)
         write(13,600)k,cmode,ctt,fuc(k),delt(k),fn(k),
     .                timem(k),exp(k)
c
         k=k+1
c
 100     continue
c
cccccc
cccccc    find mean, standard deviation and turbulence intensity (%)
cccccc
c z component
         if(nz.gt.0)then
            tn     = real(nz)
            meanuz = temuz/tn
```

```
c
            tt      = (temuz2/tn) - meanuz**2.
            if(tt.ge.0.0)then
              devuz  = dsqrt(tt)
            else
              if(tt.gt.-0.5)devuz = 0.0
              if(tt.le.-0.5)devuz = -1.0
            endif
c
            turbiz = devuz*100./meanuz
         else
            meanuz=0.
            devuz =0.
            turbiz=0.
         endif
c r component
         if(nr.gt.0)then
            tn      = real(nr)
            meanur = temur/tn
c
            tt      = (temur2/tn) - meanur**2.
            if(tt.ge.0.0)then
              devur  = dsqrt(tt)
            else
              if(tt.gt.-0.5)devur = 0.0
              if(tt.le.-0.5)devur = -1.0
            endif
c
            turbir = devur*100./meanur
         else
            meanur=0.
            devur =0.
            turbir=0.
         endif
cccccc
c
 500     format(4x,' ',4x,'mode',8x,'dir',4x,'velocity',6x,'delta t',
     .          5x,'N',6x,'time',4x,'exp',/)
 600  format(1x,I4,3X,A10,3X,A2,3X,E10.4,3X,E10.4,3X,F5.1,3X,F6.1,
     .          3X,F3.1)

write(13,700)meanuz,meanur,devuz,devur,turbiz,turbir,nz,nr,
     .                  xloc,yloc,zloc
 700     format(/,4x,'mean Uz              = ',E10.4,6x,
     .          'mean Ur             = ',E10.4,/,
     .          4x,'std dev Uz          = ',E10.4,6x,
     .          'std dev Ur          = ',E10.4,/,
     .          4x,'turb intensity z % = ',F6.2,10x,
     .          'turb intensity r % = ',F6.2,//,4x,'# data z ',
     .          I4,24x,'# data r ',I4//,4x,'x (mm) = ',F10.4,/,4x
     .          'y (mm) = ',F10.4,/,4x,'z (mm) = ',F10.4)
c
c
         rewind 12
         rewind 13
         close(12)
```

```
        close(13)
c
c
        end
c
c$$$$$$$$$$$$$$$$$$$$$$$$$$$$$$$$$$$$$$$$$$$$$$$$$$$$$$$$$$$$$$$$$$$$$$
c$$$$$$$$$$$$$$$$$$$$$$$$$$$$$$$$$$$$$$$$$$$$$$$$$$$$$$$$$$$$$$$$$$$$$$
c$$$$$$$$$$$$$$$$$$$$$$$$$$$$$$$$$$$$$$$$$$$$$$$$$$$$$$$$$$$$$$$$$$$$$$
c$$$$$$$$$$$$$$$$$$$$$$$$$$$$$$$$$$$$$$$$$$$$$$$$$$$$$$$$$$$$$$$$$$$$$$
c
        subroutine dec2bin
cccc
cccc    converts LDV data from decimal to binary for interpretation
cccc
        character*16 bit,cbit,fname,fileo,word(1024)
        real*8 numb,x,ftwo(16),fdat(1024),temp(4)
        real*4 xloc,yloc,zloc
        real*8 fshftz,fshftr
        integer*4 i,j,ksamp,nsamp
c
        common /ldvstuf/ fileo,nsamp,word,xloc,yloc,zloc,ksamp,
     .                   fshftz,fshftr
c
        data ftwo /32768.,16384.,8192.,4096.,2048.,1024.,512.,256.,
     .            128.,64.,32.,16.,8.,4.,2.,1./
cccccccccccccccccccccccccccccccccccccccccccccccccccccccccccccccccccccc
c
c  read in ldv data file
c
        write(*,'(a)')'(old) ldv data file name:'
        read(*,'(a)') fname
        open(10,file=fname,form='formatted',status='old')
c
c  make file for converted data
c
c       write(*,'(a)')' new data file name - for binary info :'
c       read(*,'(a)') fileo
        fileo='bitemp.dat'
        open(11,file=fileo,status='unknown')
c
ccccccccccccccccccccccccccccccccccccccccccccccccccccccccccccccccccccc
c
c  read in ldv data in the form :  number of samples
c                                  x,y,z (meters)
c                                  frequency shift z (Hz)
c                                  frequency shift r (Hz)
c                                  data
c                                   "
cccccccccccccccccccccccccccccccccccccccccccccccccccccccccccccccccccccc
        read(10,*)nsamp,xloc,yloc,zloc,fshftz,fshftr,
     .            (fdat(j),j=1,2*nsamp)
c
        rewind 10
        close(10)
c
c
```

```
      ksamp = 0
c
c
      do 200 j=1,2*nsamp
      bit='0000000000000000'
      cbit='1111111111111111'
      if(fdat(j).gt.0.0) goto 999
      ksamp = ksamp + 1
      numb=dabs(fdat(j))
c
c
      do 100 i=1,16
       if (numb .ge. ftwo(1))then
        write (*,*)' number greater than 2**16 !!!!!!!!'
        go to 999
       endif
       if ((numb .lt. ftwo(i)) .and. (numb .ge. ftwo(i+1))) then
        bit(i+1:i+1)='1'
        cbit(i+1:i+1)='0'
        numb=numb-ftwo(i+1)
       endif
 100   continue
c
c
       if(cbit(16:16).eq.'0')then
          cbit(16:16)='1'
          go to 150
       endif
c
       if(cbit(15:16).eq.'01') then
       cbit(15:16)='10'
       elseif(cbit(14:16).eq.'011') then
       cbit(14:16)='100'
       elseif(cbit(13:16).eq.'0111') then
       cbit(13:16)='1000'
       elseif(cbit(12:16).eq.'01111') then
       cbit(12:16)='10000'
       elseif(cbit(11:16).eq.'011111') then
       cbit(11:16)='100000'
       elseif(cbit(10:16).eq.'0111111') then
       cbit(10:16)='1000000'
       elseif(cbit(9:16).eq.'01111111') then
       cbit(9:16)='10000000'
       elseif(cbit(8:16).eq.'011111111') then
       cbit(8:16)='100000000'
       elseif(cbit(7:16).eq.'0111111111') then
       cbit(7:16)='1000000000'
       elseif(cbit(6:16).eq.'01111111111') then
       cbit(6:16)='10000000000'
       elseif(cbit(5:16).eq.'011111111111') then
       cbit(5:16)='100000000000'
       elseif(cbit(4:16).eq.'0111111111111') then
       cbit(4:16)='1000000000000'
       elseif(cbit(3:16).eq.'01111111111111') then
       cbit(3:16)='10000000000000'
       elseif(cbit(2:16).eq.'011111111111111') then
```

```
          cbit(2:16)='100000000000000'
          elseif(cbit(1:16).eq.'0111111111111111') then
          cbit(1:16)='1000000000000000'
          endif
c
 150      continue
c
c
c
c         write(*,*)'decimal = ',x,'    binary = ',bit
c         write(*,*)'binary 2"s complement = ',cbit
          write(11,*)cbit
          word(j)=cbit
c
 200     continue
c
 999     continue
         rewind 11
         close(11,status='keep')
         return
         end
```

form of data input :

number of samples
x, y, z coordinates
frequency shift - z direction
frequency shift - r direction
data...

example

input :

```
8
10 0 0
0.
0.
-16376
-16376
-16376
-32760
-3771
-16376
-3771
-16376
-16376
-3771
-16376
-3771
-16376
-3771
-16376
-3771
```

ouput :

	mode	dir	velocity	delta t	N	time	exp
1	random	z	.4128E+00	.1000E-03	8.0	3072.0	8.0
2	random	z	.6192E+00	.1000E-03	8.0	2048.0	8.0
3	random	r	.3377E+01	.4096E+00	69.0	3072.0	8.0
4	random	r	.3377E+01	.4096E+00	69.0	3072.0	8.0
5	random	z	.2628E+01	.1000E-03	8.0	3860.0	5.0
6	random	z	.2628E+01	.1000E-03	8.0	3860.0	5.0
7	random	z	.2628E+01	.1000E-03	8.0	3860.0	5.0
8	random	z	.2628E+01	.1000E-03	8.0	3860.0	5.0

mean Uz	= .1924E+01	mean Ur	= .3377E+01
std dev Uz	= .9975E+00	std dev Ur	= .0000E+00
turb intensity z %	= 51.84	turb intensity r %	= .00
# data z	6	# data r	2

x (mm) = 10.0000
y (mm) = .0000
z (mm) = .0000

TABLE 1

LDV PARAMETERS

DESCRIPTION	SYMBOL	Channel 1 Blue	Channel 2 Green
laser wavelength (nm)	λ	488.0	514.5
lens focal length (mm)	f	480.0	480.0
laser beam spacing (mm)	d	48.75	48.75
beam half angle (degrees)	Φ	2.907	2.907
fringe spacing (μm)	d_f	4.81	5.07
unfocused beam diameter(mm)	$D_{e^{-2}}$	4.875 *	4.875 *
beam diam. at focus (mm),	$d_{e^{-2}}$	0.0612	0.0645
probe volume width (mm)	d_m	0.00613	0.00646
probe volume length (mm)	l_m	1.21	1.27
probe volume (mm^3)	V	0.00237	0.00277
number of fringes	N_f	~ 13	~ 13

* De_{-2}' = 1.3 mm before beam expansion

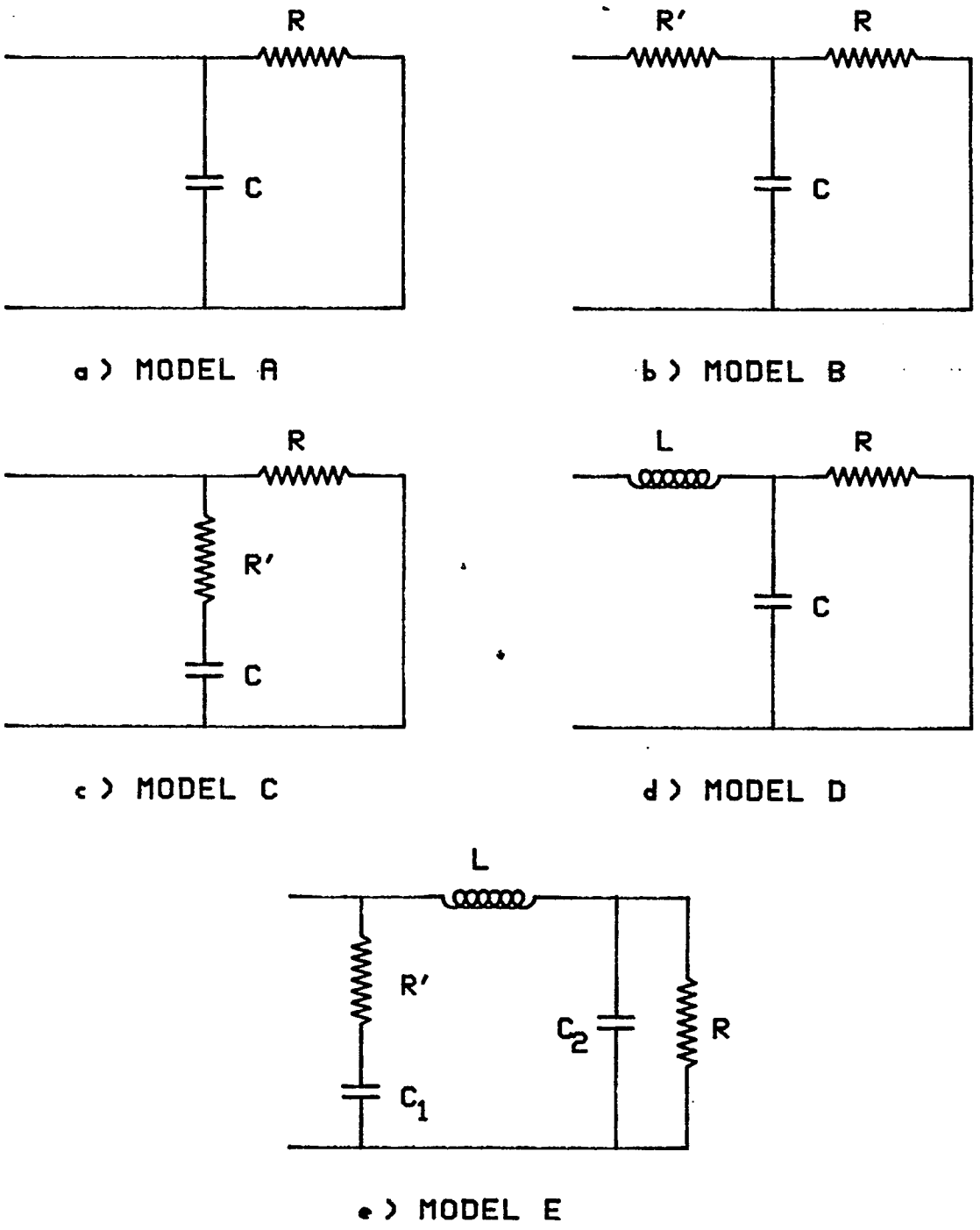

Figure 1 - Arterial System Models

SD = Systolic Interval = 0.3 seconds
SV = Stroke Volume = 75.0 ml/stroke
HR = Heart Rate = 75.0 beats/minute

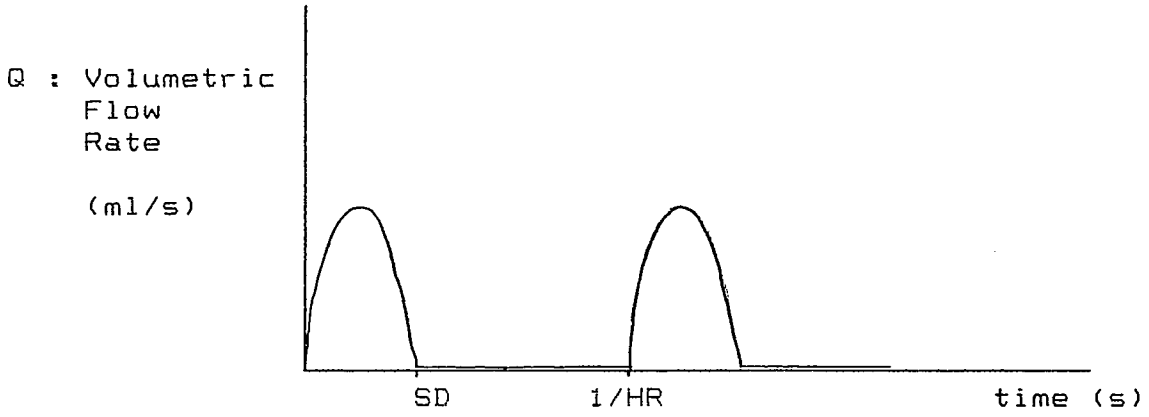

During the Systolic Interval :

$$Q = \frac{(SV/SD)\ \sin(\ \pi\ t/\ SD)}{0.636}$$

Figure 2 - Arterial Pulse Pressure Model
Flow Input

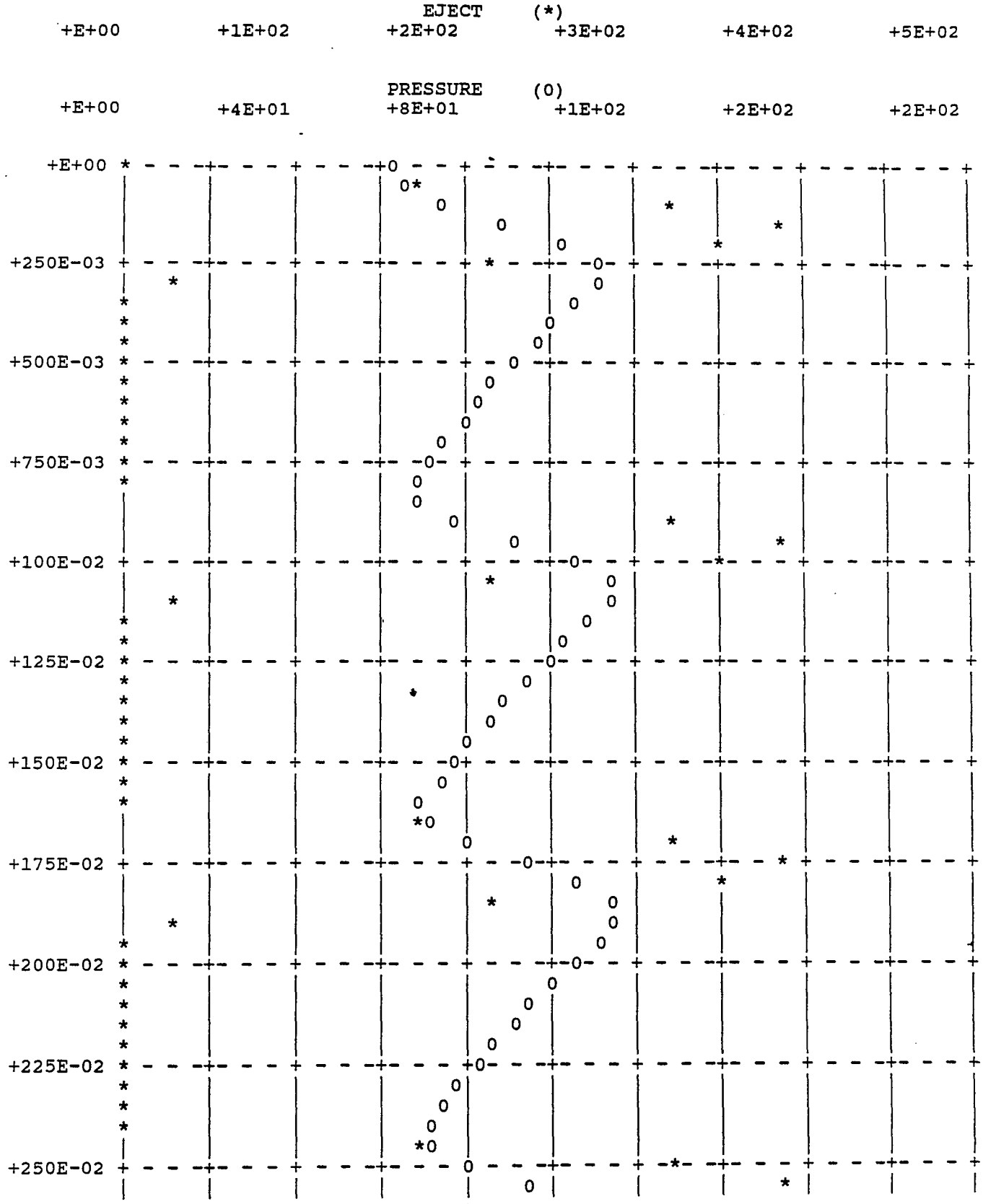

Figure 3 - Model A R = C = 1

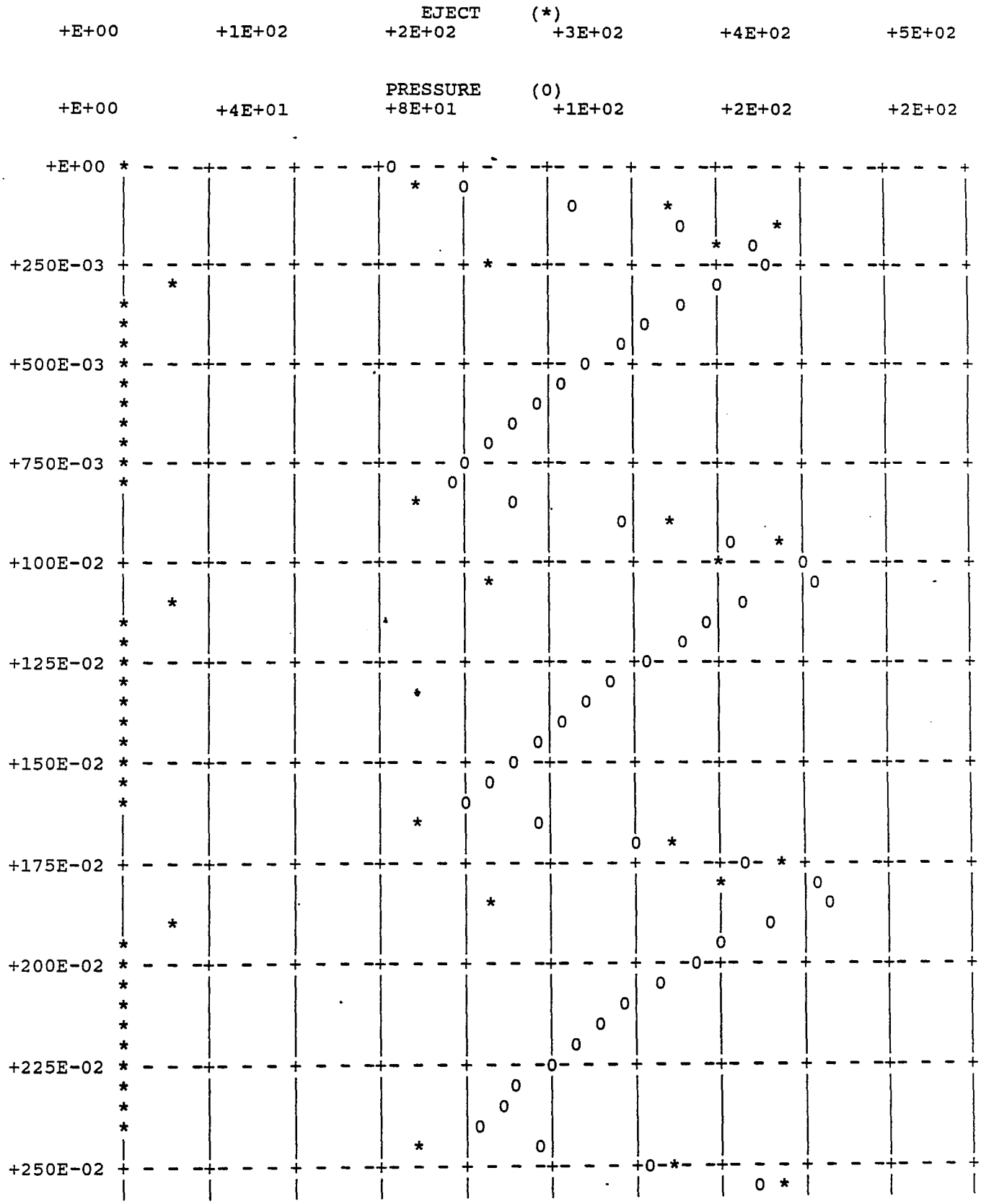

Figure 4 - Model B C=0.666 R=1.25 R'=0.075

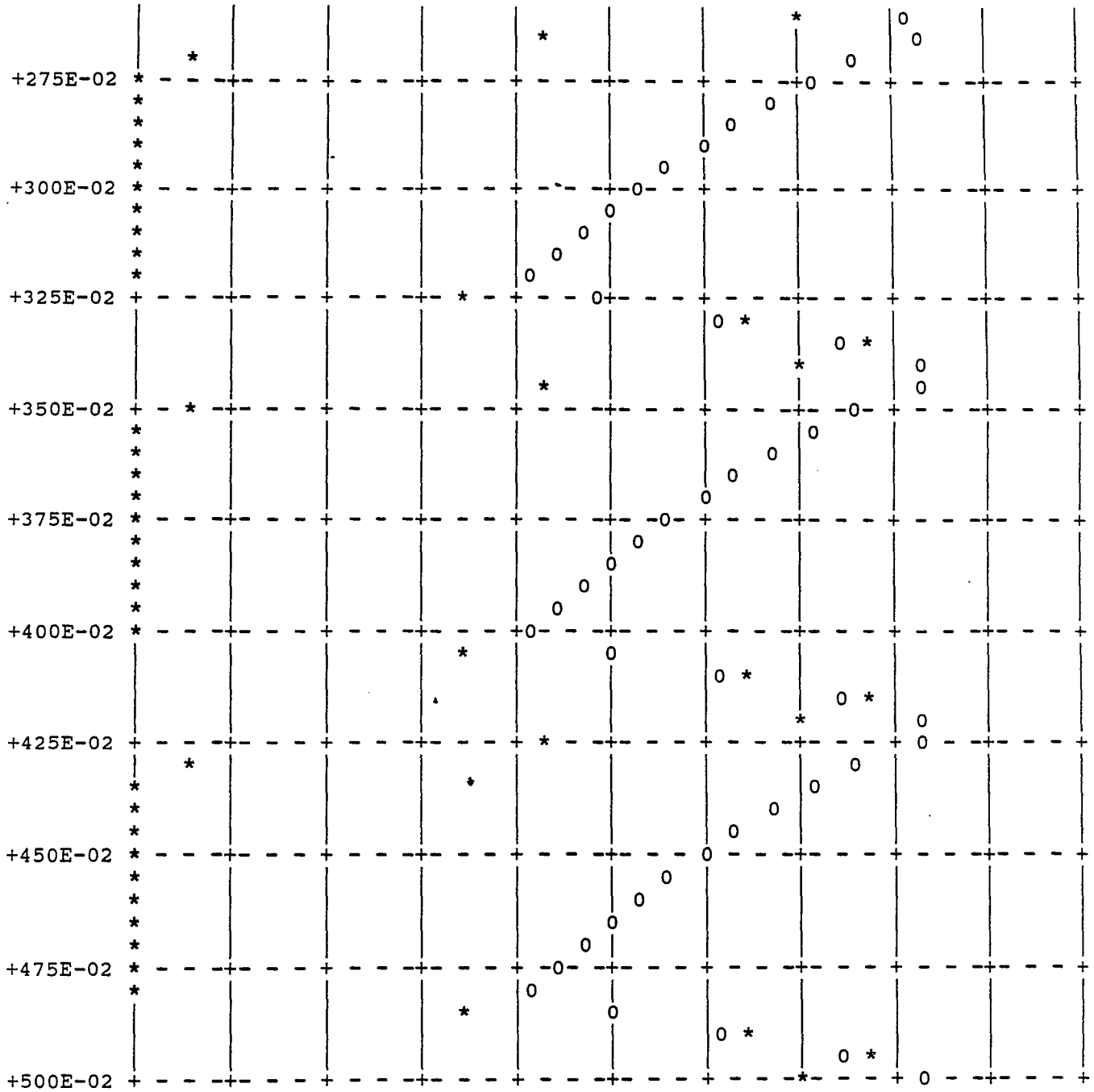

Figure 4 cont'd

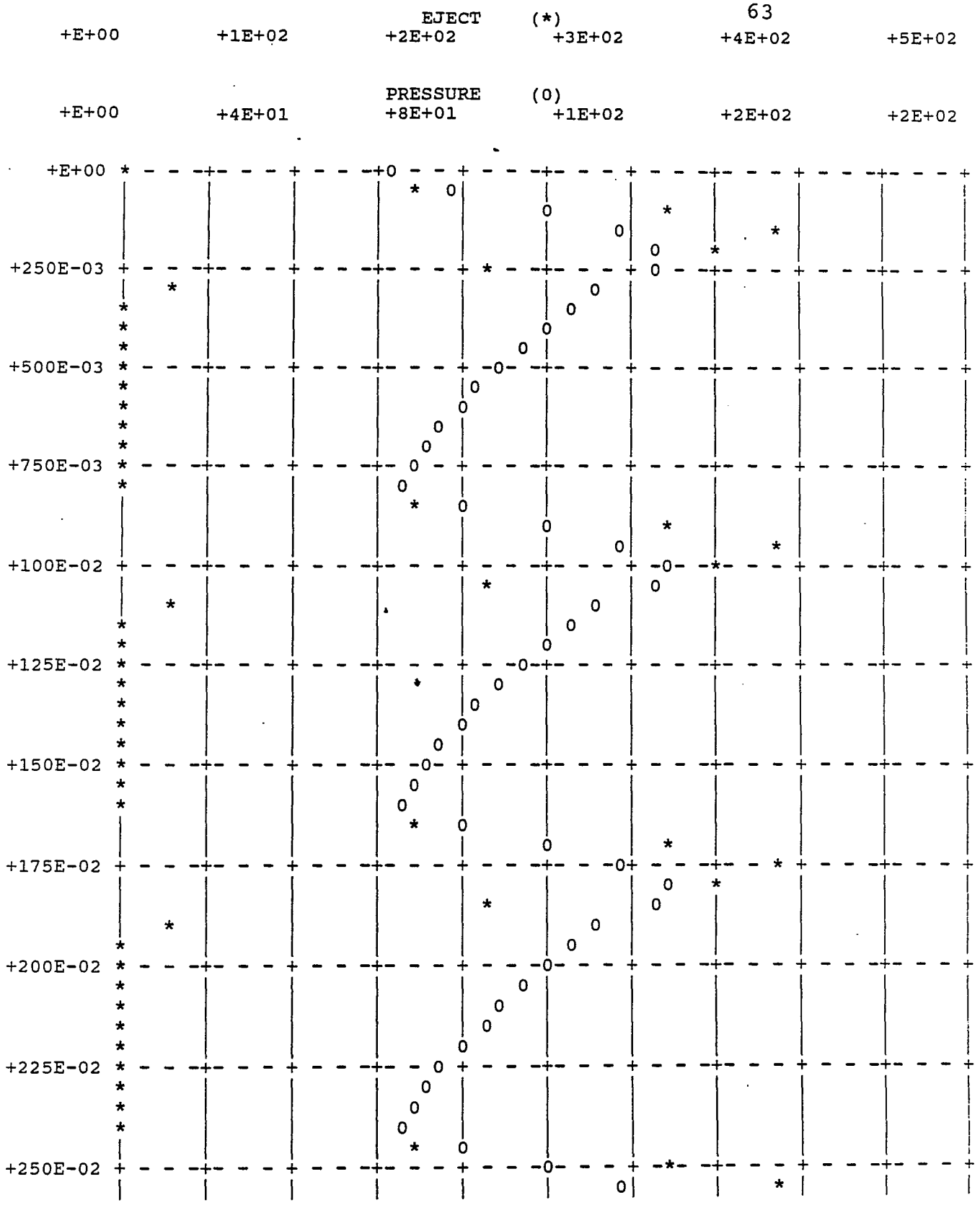

Figure 5 - Model B C=1 R=0.93 R'=0.075

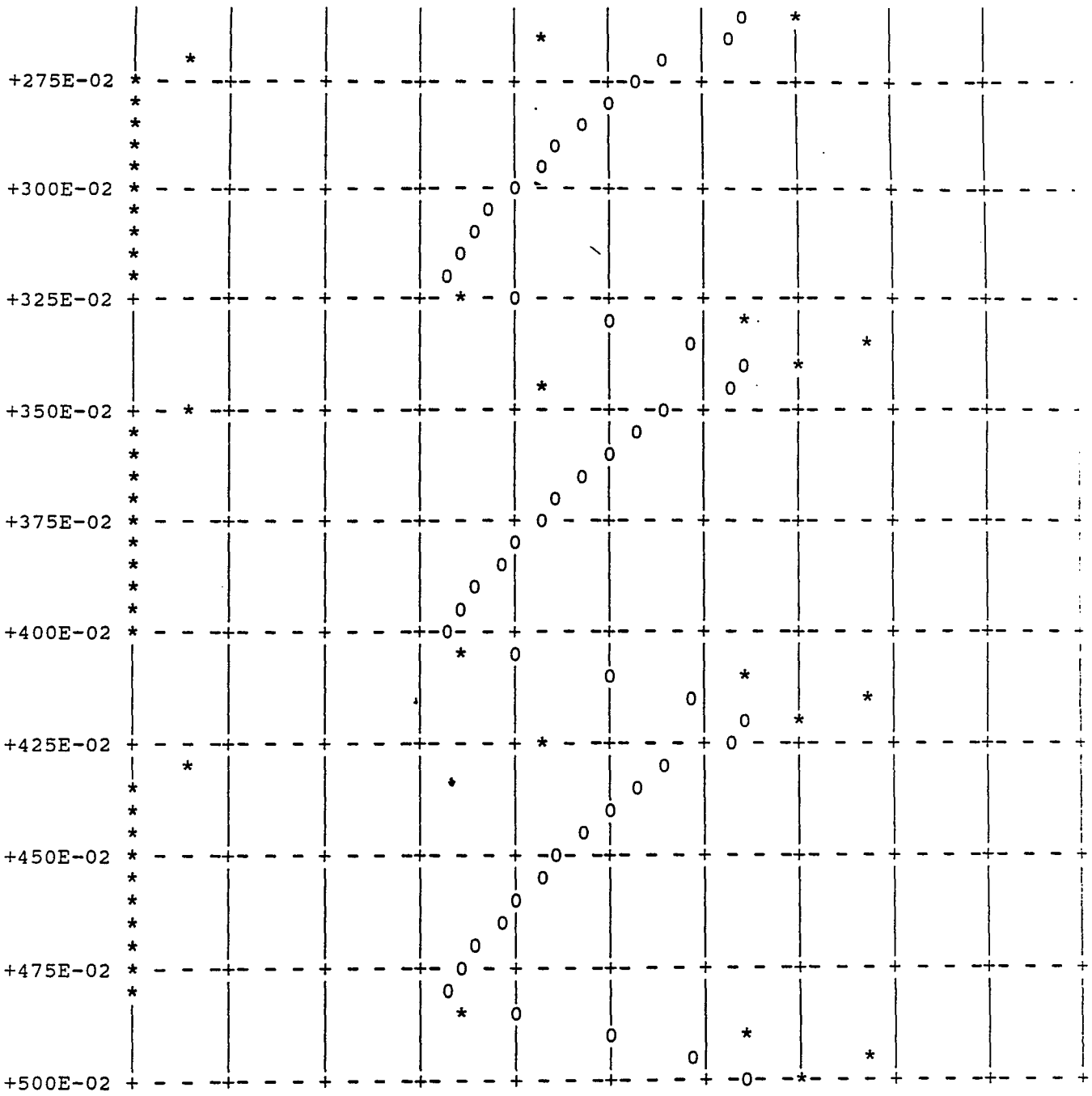

Figure 5 cont'd

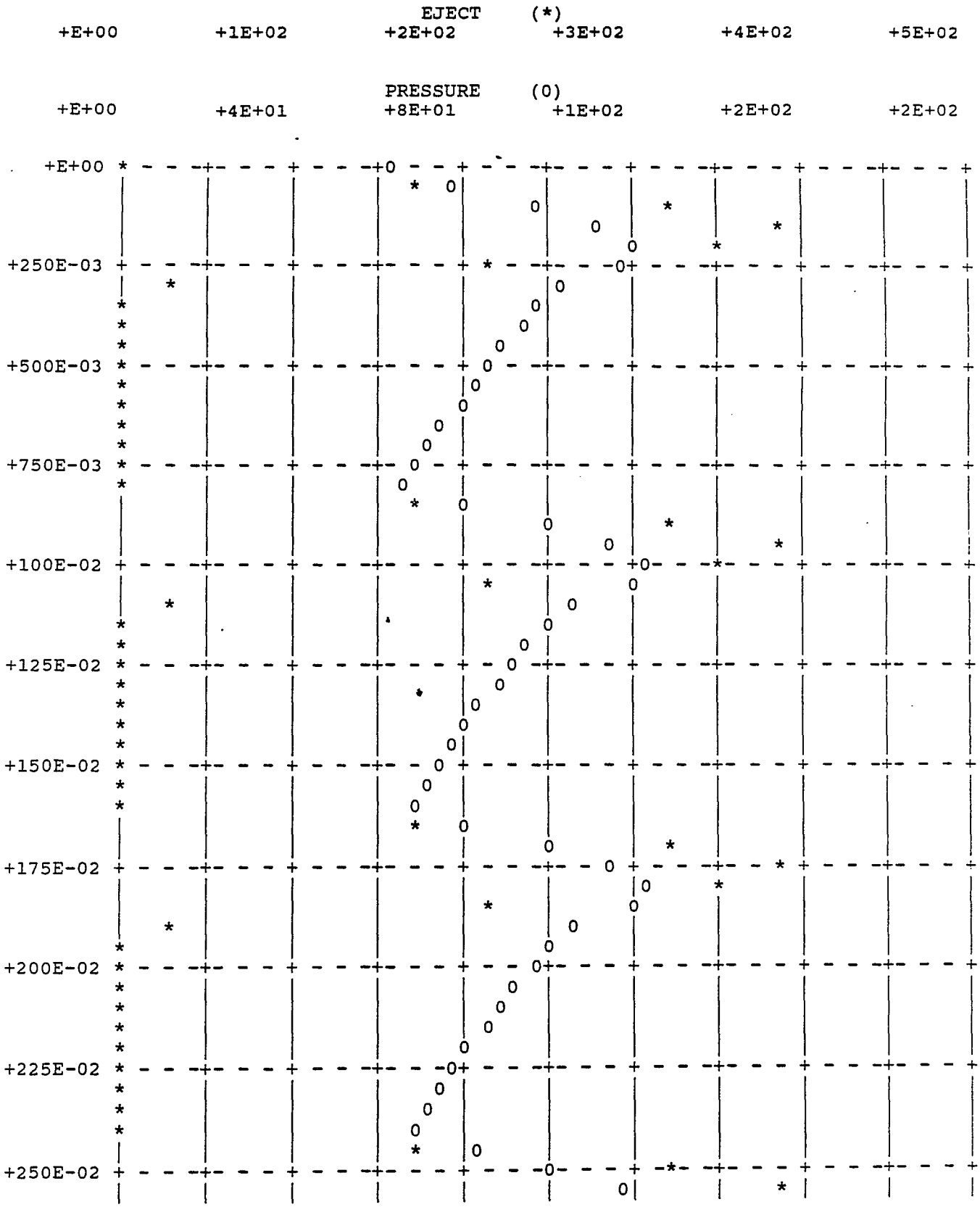

Figure 6 - Model B C=1.23 R=0.93 R'=0.075

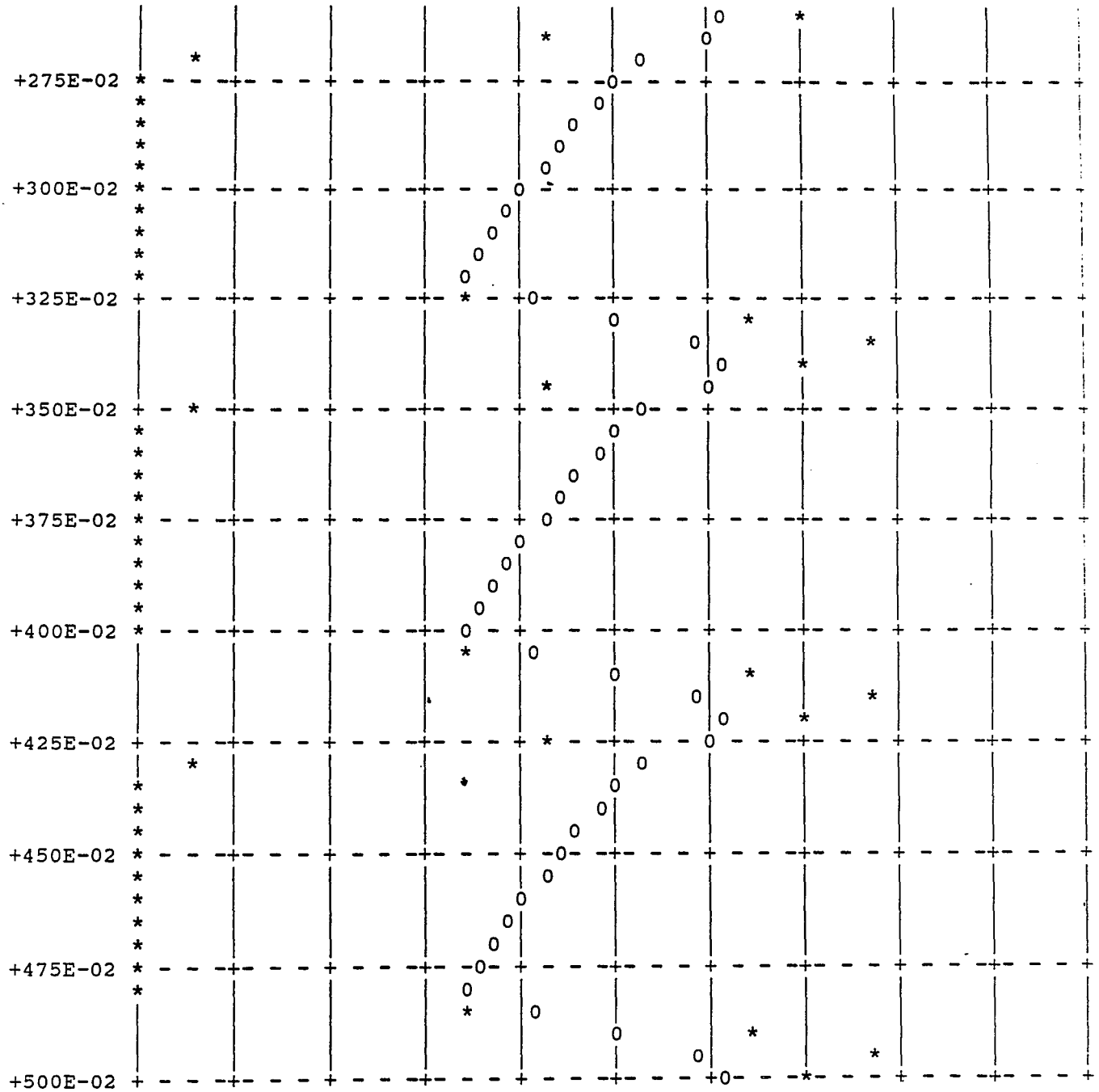

Figure 6 cont'd

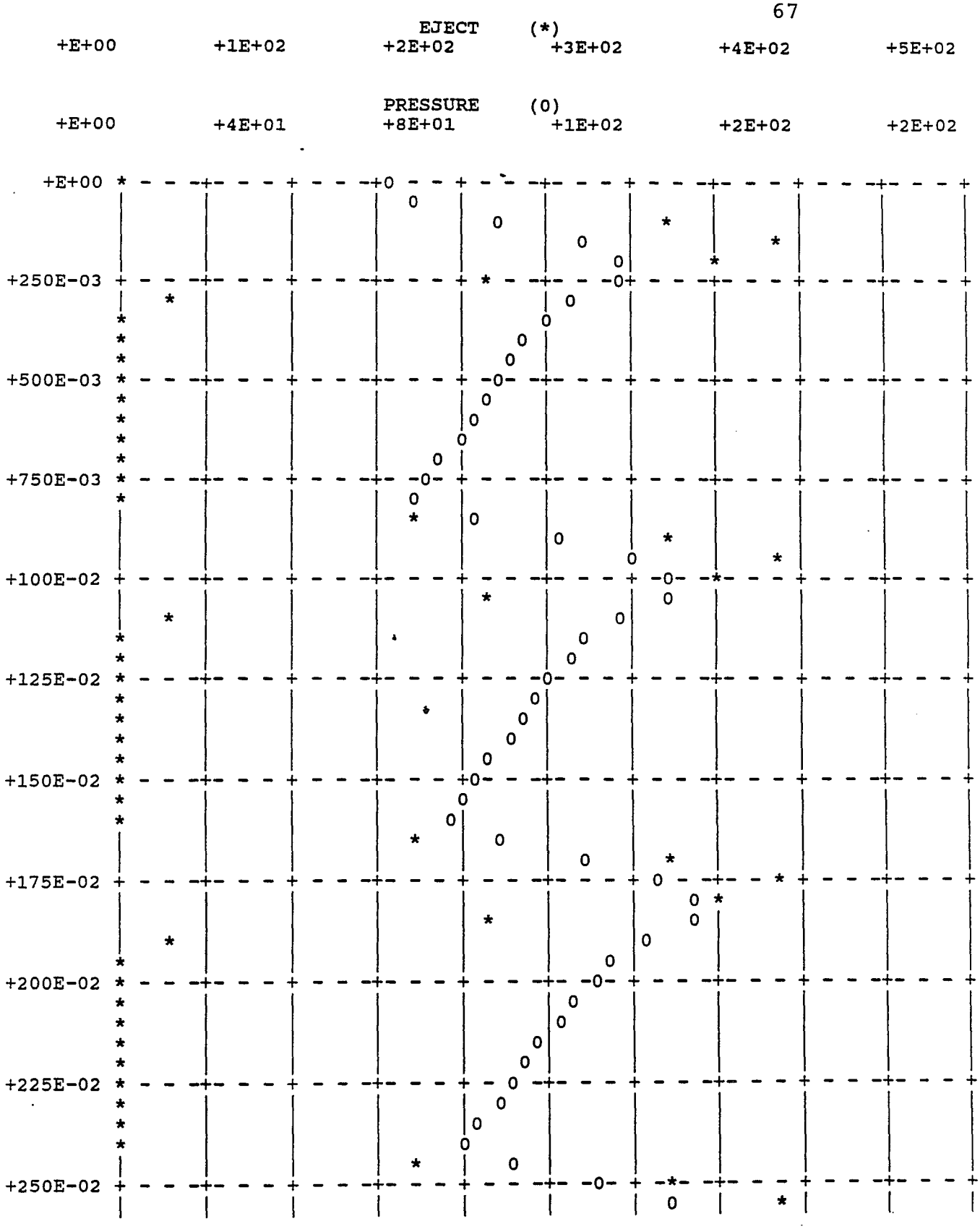

Figure 7 - Model C C=1 R=1.2 R'=0.075

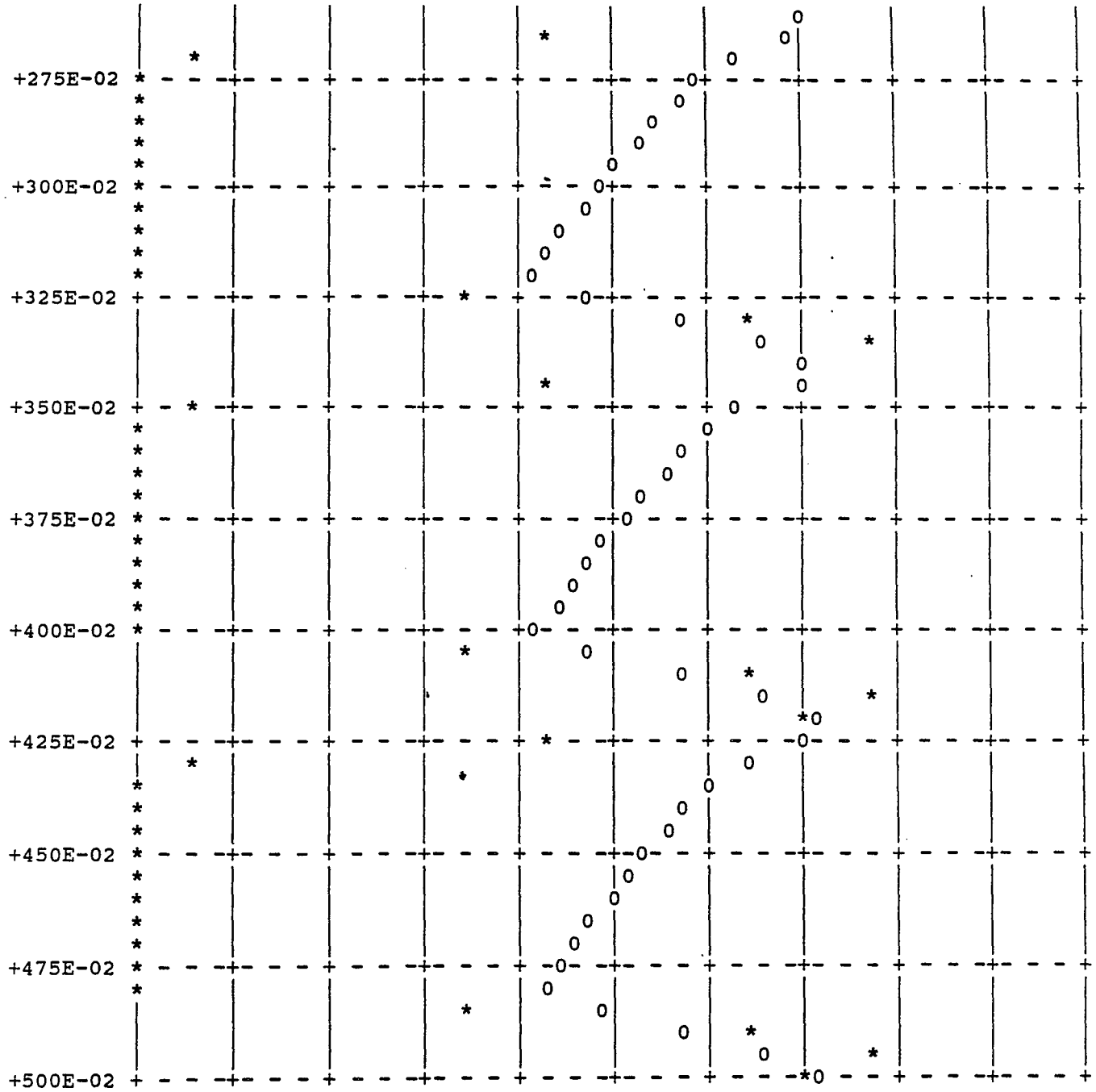

Figure 7 cont'd

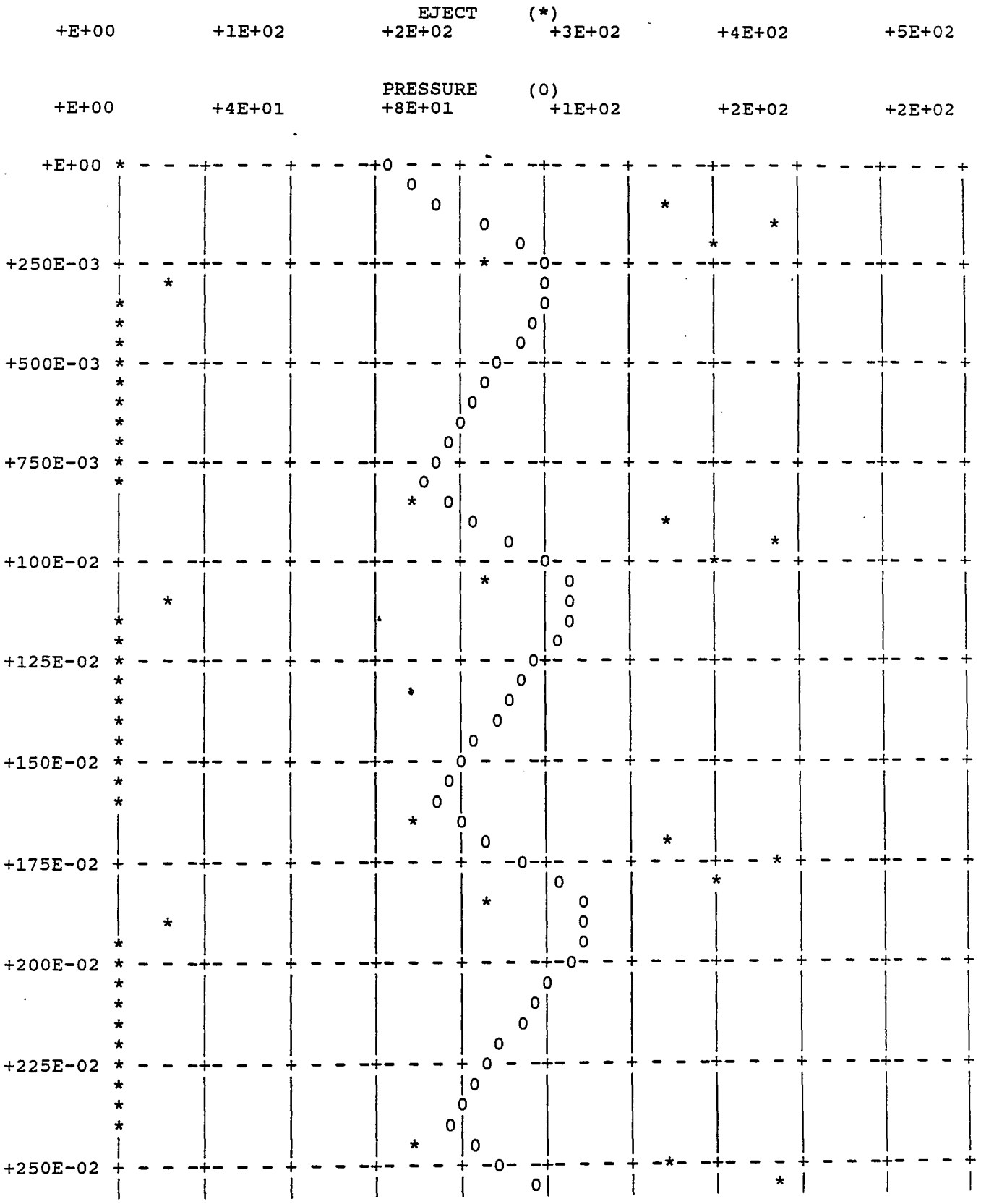

Figure 8 - Model D C=1.223 R=1.05 L=0.001

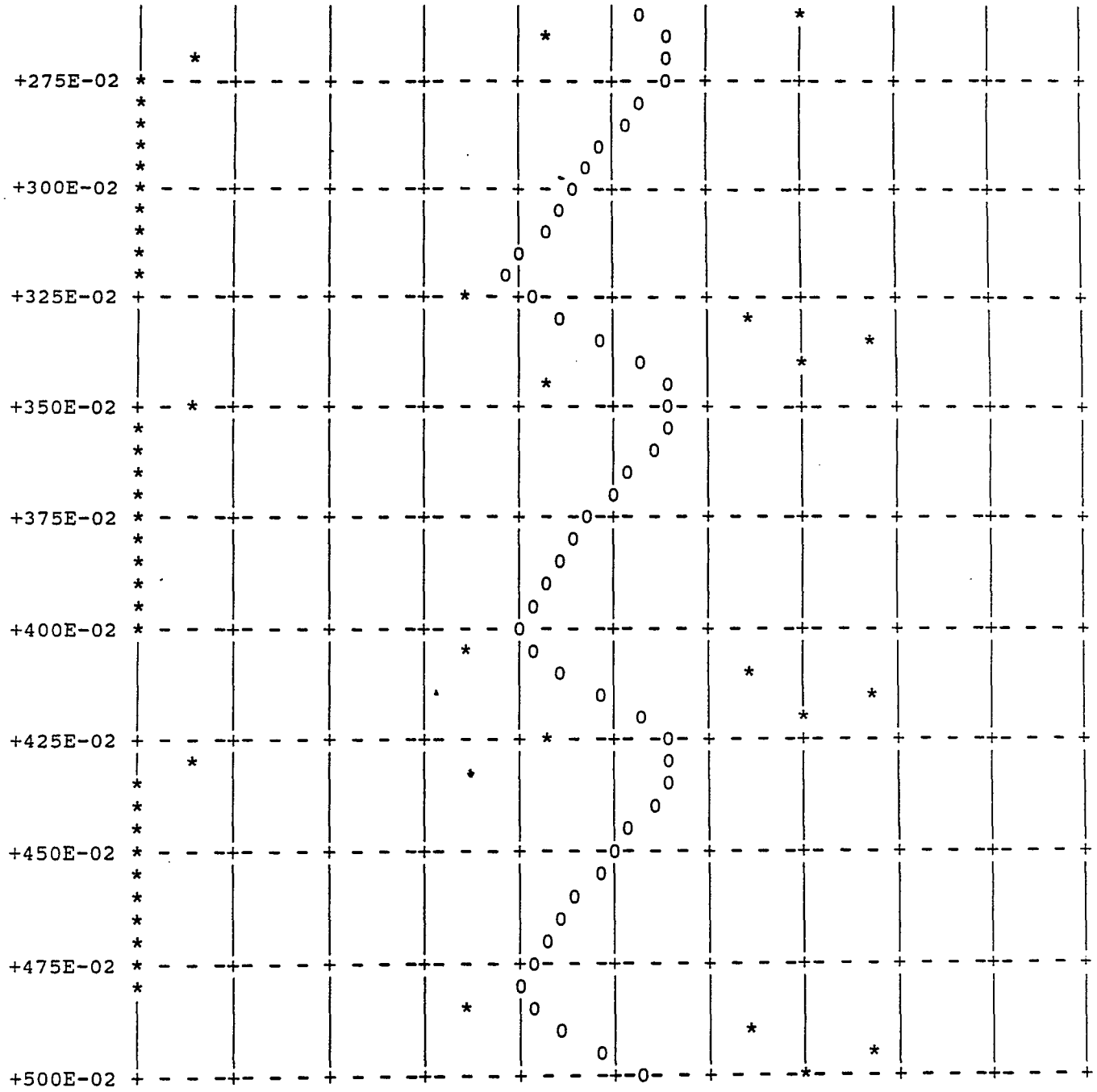

Figure 8 cont'd

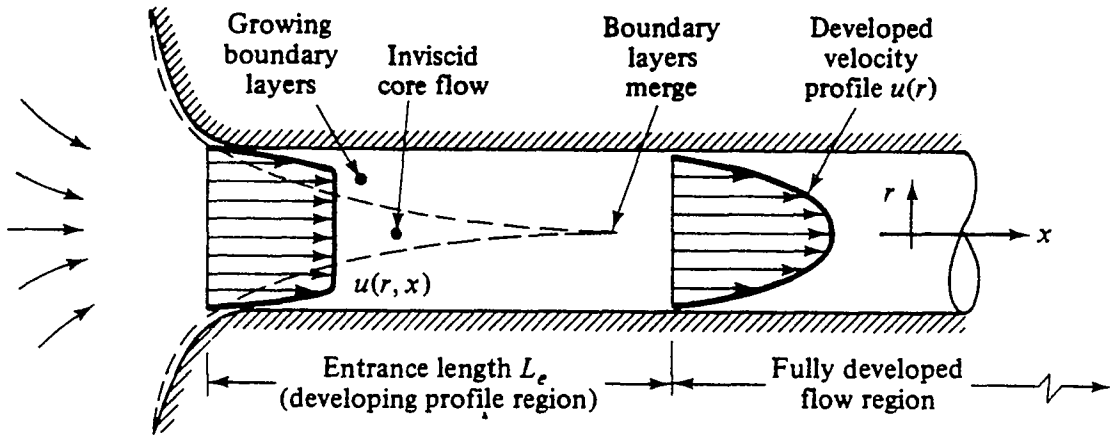

Figure 9. Entrance Length Effect (Ref. 55)

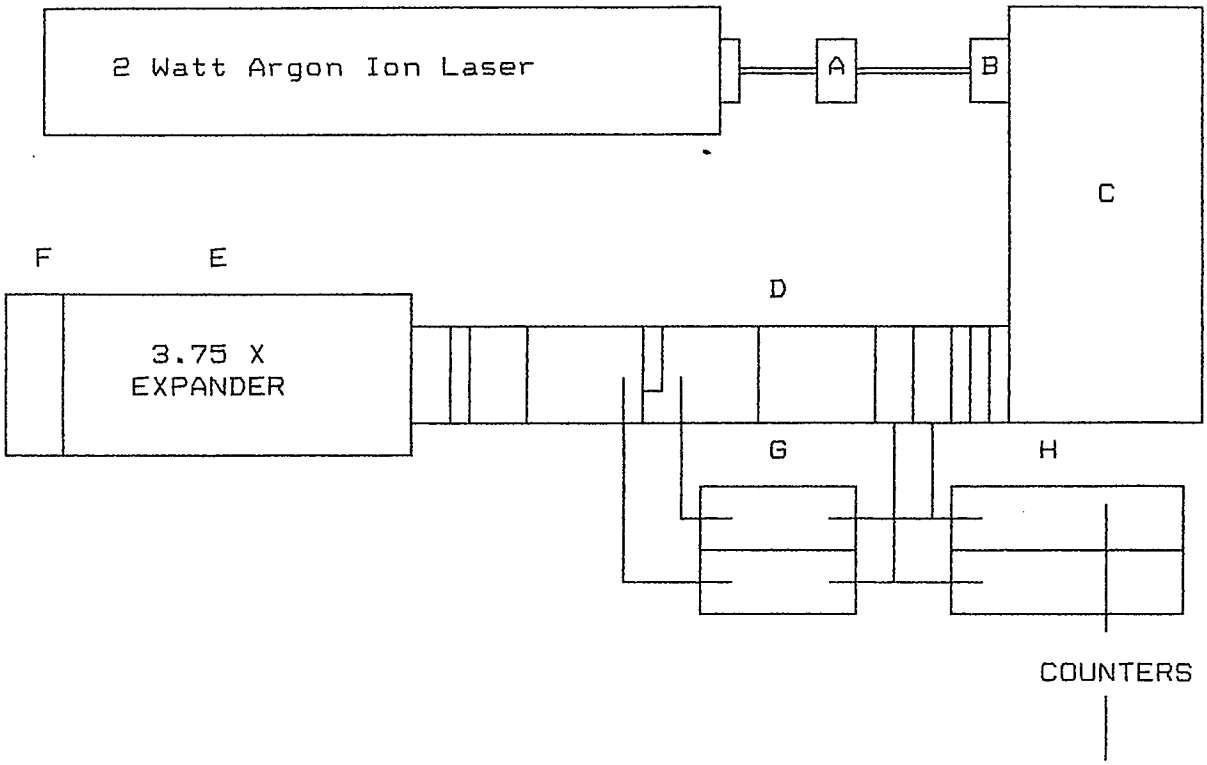

Item	Description
A	Collimator
B	Polarizer
C	Color Separator
D	Polarizer (X2) Beam Displacer (X2) Beam Splitter (X2) Frequency Shifter (Bragg Cell X2) Beam Steering Module (X2) Beam Stop Receiving Assembly - Photodetector (X2) Receiving Color Separator Beam Stop Beam Reducer (X2)
E	Beam Expander
F	Focusing Lens
G	Photodetector Power Supply
H	Frequency Shifter Control

Figure 10 - The LDV System

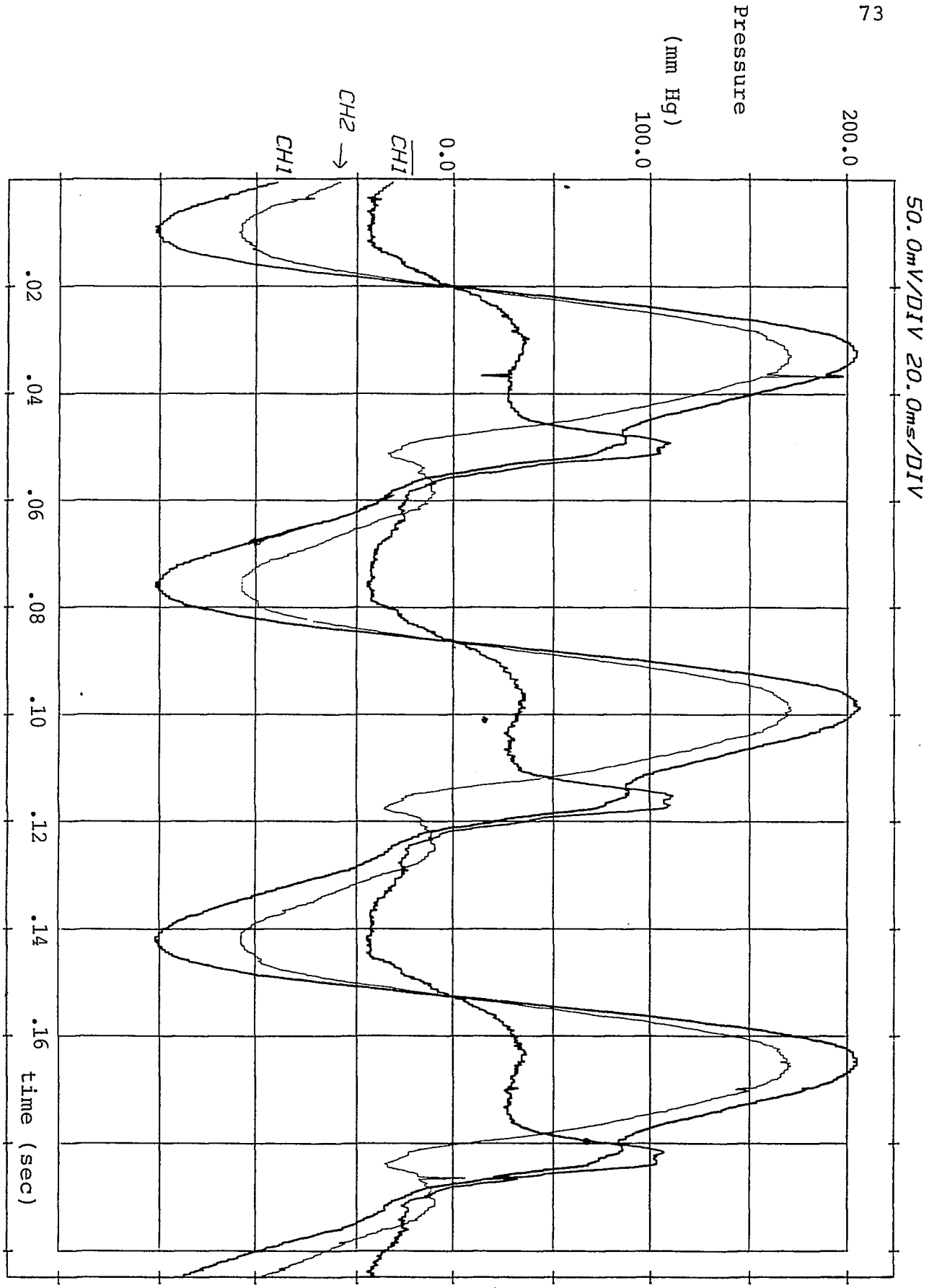

Figure 11. Pressure Measurements within an Accelerated Fatigue Tester

CH1 - Upstream Pressure, CH2 - Downstream Pressure, $\overline{CH1}$ - Delta Pressure

SELECTED BIBLIOGRAPHY

1. Alchas, P.G., Snyder, A.J. and Phillips, W.M., "Pulsatile Prosthetic Valve Flows: Laser-Doppler Studies," Biofluid Mechanics 2, p. 243, Plenum Press, 1980.

2. American Edwards Laboratories: Carpentier-Edwards Bioprostheses. Valve Brochure.

3. The Bantam Medical Dictionary. Bantam Books, 1981.

4. Barnhart, G.R., Jones, M., Ishihara, T., Chavez, A., Rose, D.M., and Ferrans, V.J., "Bioprosthetic Valvular Failure," Journal Thoracic and Cardiovascular Surgery, 83:618, 1982.

5. Bendick, P.J. and Glover, J.L., "Detection of Subcritical Stenoses by Doppler Spectrum Analysis," Surgery, 91:707.

6. Bird, R.B., Stewart, W.E. and Lightfoot, E.N., Transport Phenomena, J. Wiley and Sons, 1960.

7. Broom, N.D., "Fatigue-Induced Damage in Glutaraldehyde-Preserved Heart Valve Tissue," Journal Thoracic and Cardiovascular Surgery, 76:202, 1978.

8. Broom, N.D., "The Stress/Strain and Fatigue Behavior of Glutaraldehyde Perserved Heart-Valve Tissue," Journal of Biomechanics, 10:707, 1977.

9. Brubakk, J.E. and Aaslid, R., "Use of a Model for Simulating Individual Aortic Dynamics in Man," Medical and Biological Engineering and Computers, 16:231, 1978.

10. Carbonarro, M., Notes for the Boundary Layer Course at the von Kármán Institute for Fluid Dynamics.

11. Cen, R., Liu, B. and Hwang, N., "Developing Oscillatory Flow in a Circular Pipe: A New Solution," ASME Journal of Biomechanical Engineering, 109:340, 1987.

12. Chandran, K.B., Khalighi, B. and Chen, C.J., "Experimental Study of Physiological Pulsatile Flow Past Valve Prostheses in a Model of Human Aorta," Journal of Biomechanics, 18:10:773, 1985.

13. Clark, R.E., Swanson, W.M., Kardos, J.L., Hagen, R.W., and Beauchamp, R.A., "Durability of Prosthetic Heart Valves," The Annals of Thoracic Surgery, 26:323, 1978.

14. Cooney, D.O., Biomedical Engineering Principles, Marcel Dekker, Inc., 1976.

15. Denison, E.B., Stevenson, W.H. and Fox, R.W., "Pulsating Laminar Flow Measurements with a Directionally Sensitive Laser Velocimeter," AIChE Journal, 17:781, 1971.

16. Dinnar, U., Cardiovascular Fluid Dynamics, CRC Press, 1981.

17. Einav, S., Stolero, D., Avividor, J.M., and Elad, D., "LDA Evaluation of Wall Shear Stress Distribution Along the Cusp of a Tri-Leaflet Prosthetic Heart Valve," Laser Doppler Anemometry Conference, Lisbon, Portugal, 1988.

18. Figliola, R.S. and Meuller, T.J., "On the Hemolytic and Thrombogenic Potential of Occluder Prosthetic Heart Valves from In-Vitro Measurements," ASME Journal of Biomechanical Engineering, 103:83, 1981.

19. Gabbay, S., Kadam, P., Factor, S., and Cheung, T.K., "Do Heart Valve Bioprostheses Degenerate for Metabolic or Mechanical Reasons?," Journal Thoracic and Cardiovascular Surgery, 95:208, 1988.

20. Gabbay, S., Bortolotti, U., and Josif, M., "Mechanical Factors Influencing the Durability of Heart Valve Pericardial Bioprostheses," Transactions of the American Society of Artificial Internal Organs, 32:282, 1986.

21. Gabbay, S., Bortolotti, U., Wasserman, F.,and Factor, S., "Haemodynamics and Durability of Mitral Bioprostheses - an in vitro Study," European Heart Journal, 5:65, 1984.

22. Gabbay, S., Bortolotti, U., Wasserman, F., Factor, S., Strom, J., and Frater, R., "Fatigue-Induced Failure of the Ionescu-Shiley Pericardial Xenograft in the Mitral Position," Journal Thoracic and Cardiovascular Surgery, 87:836, 1984.

23. Gabbay, S., Bortolotti, U., Cipolletti, G., Wasserman, F., Frater, R., and Factor, S., "The Meadox Unicusp Pericardial Bioprosthetic Heart Valve: New Concept," Annals of Thoracic Surgery, 37:448, 1984.

24. Hussain, A.K.M.F., "Mechanics of Pulsatile Flows of Relevance to the Cardiovascular System," Cardiovascular Dynamics, W.B. Saunders, Philadelphia, 1970.

25. Hussain, A.K.M.F. and Reynolds, W.C., "The Mechanics of an Organized Wave in a Turbulent Shear Flow," Journal of Fluid Mechanics, 41:241, 1970.

26. Kirmse, R.E., "Investigations of Pulsating Turbulent Pipe Flow," ASME Journal of Fluids Engineering, 101:436, 1979.

27. Ku, D.N. and Giddens, D.P., "Laser Doppler Anemometer Measurements of Pulsatile Flow in a Model Carotid Bifurcation," Journal of Biomechanics, 20:4:407, 1987.

28. Lieber, B.B. and Giddens, D.P., "Apparent Stresses in Disturbed Pulsatile Flows," Journal of Biomechanics, 21:287, 1988.

29. Lieber, B.B., Giddens, D.P., Kitney, R.I., and Talhami, H., "On the Discrimination Between Band-Limited Coherent and Random Apparent Stresses in Transitional Pulsatile Flow," ASME Journal of Biomechanical Engineering, 111:42, 1989.

30. Liepsch, D., Poll, A., Stigberger, J., Sabbah, H.N., and Stein, P.D., "Flow Visualization Studies in a Mold of the Normal Human Aorta and Renal Arteries," ASME Journal of Biomechanical Engineering, 111:222, 1989.

31. Matsuzaki, Y. and Matsumoto, T., "Flow ina a Two-Dimensional Collapsible Channel with Rigid Inlet and Outlet," ASME Journal of Biomechanical Engineering, 111:180, 1989.

32. Nakamura, M. and Sawada, T., "Numerical Study on the Flow of a Non-Newtonian Fluid Through an Axisymmetric Stenosis," ASME Journal of Biomechanical Engineering, 110:137, 1988.

33. Nandy, S. and Tarbell, J.M., "Flush Mounted Hot Film Anemometer Measurement of Wall Shear Stress Distal to a Tri-leaflet Valve for Newtonian and Non-Newtonian Blood Analog Fluids," Biorheology, 24:483, 1987.

34. Ohba, K., Sakurai, A. and Oka, J., "Laser Doppler Measurement of Local Flow Field in Oscillation Collapsible Tube," Laser Doppler Anemometry Conference, Lisbon, Portugal, 1988.

35. Oka, S., Cardiovascular Hemorheology, Cambridge University Press, 1981.

36. Pollack, G.H., Reddy, R.V. and Noordergraaf, A., "Input Impedance, Wave Travel, and Reflections in the Human Pulmonary Arterial Tree: Studies Using an Electrical Analog," IEEE Transactions of Biomedical Engineering, p. 151, July 1968.

37. Ramaprian, B.R. and Tu, S., "An Experimental Study of Oscillatory Pipe Flow at Transitional Reynolds Numbers," Journal of Fluid Mechanics, 100:513, 1980.

38. Ramaprian, B.R. and Tu, S., "Fully Developed Periodic Turbulent Pipe Flow, Parts 1 and 2," Journal of Fluid Mechanics, 137:31, 1983.

39. Randall, J.E., Microcomputers and Physiological Simulation, Addison-Wesley Publishing Co., 1980.

40. Richards, C.W., Engineering Materials Science. Brooks/Cole Publishing Co, Monterey, CA, 1961.

41. Roschke, E.J. and Harrison, E.C., "Fluid Shear Stress in Prosthetic Heart Valves, Journal of Biomechanics, 10:299, 1977.

42. Schoen, F.J., and Hobson, C.E., "Anatomic Analysis of Removed Prosthetic Heart Valves: Causes of Failure of 33 Mechanical Valves and 58 Bioprostheses, 1980 to 1983," Human Pathology, 16:549, 1985.

43. Schlichting, H., Boundary Layer Theory, McGraw-Hill, 1979.

44. Schuster, P.R., and Wagner, J.W., "A Preliminary Durability Study of Two Types of Low-Profile Pericardial Bioprosthetic Valves Through the Use of Accelerated Fatigue Testing and Flow Characterization," Journal of Biomedical Materials Research, 23:207, 1989.

45. Schwarz, A.C., Tiederman, W.G. and Phillips, W.M., "Influence of Cardiac Flow Rate on Turbulent Shear Stress from a Prosthetic Heart Valve," ASME Journal of Biomechanical Engineering, 110:123, 1988.

46. Shemer, L., Wygnanski, I. and Kit, E., "Pulsating Flow in a Pipe," Journal of Fluid Mechanics, 153:313, 1985.

47. Stein, P.D., Sabbah, H.N., and Walburn, F.J., "Blood Flow Disturbances in the Cardiovascular System: Significance in Health and Disease," Biofluid Mechanics 2, p. 211, Plenum Press, 1980.

48. Stein, P.D., Walburn, F.J. and Sabbah, H.N., "Turbulent Stresses in the Region of Aortic and Pulmonary Valves," ASME Journal of Biomechanical Engineering, 104:238, 1981.

49. Sun, Y. and Gerwitz, H., "Characterization of the Coronary Vascular Capacitance, Resistance and Flow in Endocardium and Epicardium Based on a Nonlinear Analog Model," IEEE Transactions of Biomedical Engineering, 34:817, 1987.

50. Toy, S.M., Melbin, J. anf Noordergraaf, A., "Reduced Models of Arterial Systems," IEEE Transactions of Biomedical Engineering, 32:174, 1985.

51. Viedma, A., Martinez-Val, R. and Cuerno, C., "Structure of the Pulsating Flow Past Aortic Prostheses by LDA Measurements," Laser Doppler Anemometry Conference, Lisbon, Portugal, 1988.

52. Walburn, F.J. and Stein, P.D., "Wall Shear Stress During Pulsatile Flow Distal to a Normal Porcine Aortic Valve," Journal of Biomechanics, 17:2:97, 1984.

53. Walley, V.M., Bédard, P., Brais, M., and Keon, W.J., "Valve Failure Caused by Cusp Tears in Low-Profile Ionescu-Shiley Bovine Pericardial Bioprosthetic Valves," Journal Thoracic and Cardiovascular Surgery, 93:583, 1987.

54. Walley, V.M., and Keon, W.J., "Patterns of Failure in Ionescu-Shiley Bovine Pericardial Bioprosthetic Valves," Journal Thoracic and Cardiovascular Surgery, 93:925, 1987.

55. White, F.M., Fluid Mechanics, McGraw-Hill, 1979.

56. Woo, Y., Williams, F.P. and Yoganthan, A.P., "In-Vitro Fluid Dynamic Characteristics of the Abiomed Trileaflet Heart Valve Prosthesis," ASME Journal of Biomechanical Engineering, 105:338, 1983.

57. Yoganathan, A. and Concoran, W.H., "In Vitro Velocity Measurements in the Vicinity of Aortic Prostheses," Journal of Biomechanics, 12:135, 1979.

58. Yoganathan, A., Woo, Y. and Sung, H., "Turbulent Shear Stress Measurements in the Vicinity of Aortic Heart Valve Protheses," Journal of Biomechanics, 19:6:433, 1986.